QUANTIFICATION OF SALT MARSH CARBON STOCKS:

INTEGRATION OF REMOTE SENSING DATA AND TECHNIQUES

WITH FIELD MEASUREMENTS

A Dissertation

by

RANJANI WASANTHA KULAWARDHANA

Submitted to the Office of Graduate and Professional Studies of
Texas A&M University
in partial fulfillment of the requirements for the degree of

DOCTOR OF PHILOSOPHY

Chair of Committee,	Rusty A. Feagin
Co-Chair of Committee,	Sorin C. Popescu
Committee Members,	Thomas W. Boutton
	Roél López
Head of Department,	David D. Baltensperger

December 2013

Major Subject: Ecosystem Science and Management

Copyright 2013 Ranjani Wasantha Kulawardahana

ABSTRACT

Recent climatic change projections have increased scientific and public attention on the issues relating to carbon cycling patterns, its controls, and the importance of ecosystems in the cycling and sequestration process. Global carbon studies, however, primarily have focused on dry land ecosystems that extend over large areas and have not accounted for the relatively small and scattered, though highly carbon rich, ecosystems such as mangrove swamps and salt marshes. Using data from a *Spartina alterniflora* dominated salt marsh in Galveston, Texas this study integrates remote sensing data (multispectral and Light Detection and Ranging - lidar) with field measurements for the quantification of carbon pools in salt marsh ecosystems.

Findings in this study show the capability of remote sensing data for the characterization of salt marsh terrain and vegetation heights and the estimation of above-ground biomass quantities. The best biomass prediction models using lidar heights reported considerably low errors, i.e. the percent root square errors (% RSEs) are close to 20%, which is the recommended error threshold for remote sensing based forest biomass prediction models. Our findings also demonstrate that lidar as compared to spectral data can provide better estimates of above-ground biomass and carbon, even in the herbaceous and low-relief context of a salt marsh.

A clear zonation of terrain, vegetation characteristics and the distribution of biomass quantities within the marsh extent was also observed. Distribution of biomass quantities revealed linkages with the elevation. Variations in soil properties (i.e. carbon

and bulk density) in the soil profile were linked to the temporal changes in soil carbon accumulations on the marsh surface, relative sea level history and resulting vegetation transitions as corroborated by historical aerial images. In general, the amounts of soil carbon stored in recently established *Spartina alterniflora* intertidal marshes were significantly lower than those that have remained in situ for a longer period of time. These findings indicate that, even though salt marshes can respond to relative sea level rise by migrating landward, their status as a carbon sink varies as a function of both space and time. Thus, in order to predict carbon in a wetland, researchers need to know not only the elevation, the relative sea level rise rate, and the accretion rate – but also the history of land cover change and vegetation transition.

Findings of this study contribute to carbon quantification efforts in these vulnerable ecosystems. Further, these findings will also contribute to the increased understanding of the capabilities of remote sensing datasets and techniques for the quantification of these important carbon stocks.

DEDICATION

To our loving son, Yashodha

ACKNOWLEDGEMENTS

Though only my name appears on the cover of this dissertation, a great many people contributed in many different ways to its production. I owe my gratitude to all those people who have made this dissertation possible and because of whom my graduate experience has been one that I and my family will cherish forever.

First and foremost my sincere gratitude is to my advisor Dr. Rusty A. Feagin for his guidance, understanding, patience, and encouragement throughout the course of this research as well as during various hardships of my time as a graduate student at the Department of Ecosystem Science and management at Texas A & M. I am also privileged to have Dr. Sorin C. Popescu as my co-advisor. Both of them always encouraged me to explore on my own while providing the guidance to recover when my steps faltered. The mentorship that both of them provided me during different times and in different aspects of my graduate life was paramount in providing me with a well-rounded experience professionally, as well as personally. I also thank my committee members Dr. Thomas W. Boutton and Dr. Roel Lopez for their mentorship and guidance throughout the course of this research.

I am also indebted to Dr. Robert Washington-Allen for introducing me to the Aggie family and to the Department of Ecosystem Science and Management. His contributions for getting me here opened the doors for my success at TAMU. I also thank him for providing me the financial support through various assistantships to cover the academic expenses of my first three years at TAMU. I am also grateful to various

other faculty members of my department for being excellent mentors and creating a positive experience throughout my graduate life at the department. Among many others, Drs. Thomas Boutton, Steve Whisenant, Mort Kothmann, and Mark Tjoelker reserve a special place in my memory of the department for their kindness and mentorship beyond my classroom experiences with them.

I owe a great deal of appreciation to various sources of financial support during the time of this dissertation. I am grateful to the financial supports of two fellowships: Tom Slick Senior Graduate Fellowship from the College of Agriculture and Life Sciences at TAMU, and the Schlumberger Faculty for Future Fellowship from the Schlumberger Foundation Inc. that supported my academic as well as living expenses during the last two years of this dissertation work. I also acknowledge financial support from Texas AgriLife Research that covered the expenses during my first three years, the NASA New Investigator grant (NNX08AR12G), and various other support from my department in the form of assistantships and awards.

My friends at the department supported me at different points of time during this dissertation work. Among many others, I owe a very special thanks to Ricardo Colon-Rivera and Trevor Pattillo for their hard work during field data collection. I am also thankful to Shruthi Srinivasan and Ryan Sheridan for their help with lidar data processing, and to Andy Crane and Timothy Rogers for their support in processing and analyzing field samples. Thanks also go to all my other friends and colleagues and staff of the ESSM department for making my time at the department a great experience. I also cannot forget the staff members at the university apartments, Mrs. Joni Page Cook, Mrs.

Kate Kiernat and Mr. Paul Obiazi for their various support and kindness in making our lives memorable and enjoyable at the university apartments.

I have a special place in my memory for a great number of people who have consistently provided me support and professional growth opportunities. In particular, I would like to extend my profound gratitude to a few of them who opened my mind to think about graduate studies in the US; Dr. Raymond Torres of the University of South Carolina who invited me to the US; Dr. Prasad Thenkabail, my previous supervisor at the International Water Management Institute; and Dr. Keerthi Mohotti of the Tea Research Institute of Sri Lanka, my first mentor in scientific research. I also owe a great deal of gratitude to Professor Ranjith Premalal De Silva, my previous academic advisor and more importantly my role model, for his continuous guidance, encouragements, and morale support over the past 10 years period. They always foresaw my success in academic career and patiently guided me to develop professionally as well as personally. Without their encouragement and guidance, I would rather have chosen a different path in my career.

Finally my affectionate gratitude is to my beloved late father D. T. Kulawardhana, the one who taught me the incredible value of persistence, mother, two sisters, brother, my three nephews Tharindu, Dinindu, and Nithila, and my niece Vinuji for their unconditional love and patience regardless of my negligence. More than anyone else, the two strong men of my life, my husband Wipula and our son Yashodha walked all the way with me towards the completion of this dissertation, patiently tolerated all my swinging moods, listened to my sad stories and gifted me the boundless

love and caring to make me the person I am today. I owe a great deal of gratitude for both of you for all your sacrifices throughout the course of this work.

TABLE OF CONTENTS

Page

LIST OF FIGURES

Page

LIST OF TABLES

Page

1. INTRODUCTION

Coastal salt marshes provide a wide range of ecosystem services. One of these services is their ability to sequester atmospheric carbon dioxide, through mechanisms of high plant biomass production, ongoing sedimentary carbon deposition, and relatively low decay rates (Choi *et al.* 2001). Recent climatic change projections have increased scientific and public attention on the issues relating to carbon cycling patterns, its controls, and particularly the status of an ecosystem in the cycling and sequestration process. Global carbon studies, however, primarily have focused on dry land ecosystems that extend over large areas and have not accounted for the many small, scattered carbon-storing ecosystems such as mangrove swamps and salt marshes (Atjay *et al*. 1979; Olson *et al*. 1983). Terrestrial and marine environments are currently absorbing about half of the carbon dioxide that is emitted by fossil-fuel combustion (Schimel *et al*. 2001) and act as a substantial sink for atmospheric carbon dioxide. Coastal wetlands, including salt marshes, cover less than 1% of the Earth surface (Duarte *et al*. 2005; Nellemann *et al.* 2009), yet comprise approximately 25% of the global soil carbon sink (Chmura *et al*. 2003). They are among the most productive ecosystems on earth (Castillo *et al*. 2010) and thus, play an important role in global carbon cycle (Dixon 1995). In general, their rates of carbon sequestration are an order of magnitude higher than that of comparably-sized rainforests (Bridgham *et al*. 2006; McLeod *et al*. 2011; Nellemann *et al.* 2009). However, findings of previous studies in coastal salt marsh environments highlight remarkable variations in their biomass accumulation rates,

indicating uncertainties in their carbon sequestration rates, both spatially and temporarily (Mcleod *et al*. 2011; Mendelssohn and Morris 2000; Castillo *et al*. 2010).

Productivity of salt marshes is also recognized as a primary indicator of ecosystem health (Leibowitz and Brown 1990). However, over the past decades, a rapid decline in their health as well as spatial extents (Bridgham *et al*. 2006) have created a need for better understanding these carbon pools and their roles in the ecosystem functioning. Recent reports by the United Nations Environment Program (Nellemann *et al*. 2009) and the International Union for the Conservation of Nature (Laffoley and Grimsditch 2009) have stimulated international interest in the carbon stored in tidal salt marshes and other coastal ecosystems. These reports further highlight threats to the sustainability of these ecosystems.

As intertidal systems, coastal salt marshes are threatened by increasing sea level rise resulting from global warming. Rising sea levels require that marsh soils accrete vertically to maintain their position in the tidal frame (DeLaune *et al*. 1983, 1987; Warren and Niering 1993; Morris *et al*. 2002; Stralberg *et al*. 2011). A major factor in marsh accretion and migration of marsh vegetation to adjacent land areas is the plant vegetative growth (McCaffrey and Thomson 1980; Nyman *et al*. 2006), which is also responsible for atmospheric carbon dioxide sequestration. However, in many areas, the marsh vegetation that is responsible for maintaining their surface elevations through vertical accretion may not survive increased flooding periods and submergence will result in the loss of formerly productive low marsh (DeLaune *et al*. 1983; Kirwan and Temmerman 2009; Cahoon and Reed 1995). In some areas local subsidence due to

geologic faults activated by anthropogenic activities, including extraction of sub surface hydrocarbons (White and Morton 1997) and ground water (Holzer and Galloway 2005) have aggravated the submergence and thus the loss of salt marshes. Further, these resource rich environments have increasingly attracted anthropogenic development in these coastal environments resulting further loss of marshes (Silliman *et al*. 2009). These changing environments over the past decades therefore, have collectively built up increased pressure on these coastal environments and threaten the permanence or sustainability of the marsh and the carbon it stores. Therefore, it is essential to determine their sustainability and permanence as carbon sinks.

Because of the challenge that climate change presents to these environments, these wetland ecosystems have received increased research attention, particularly to investigate their roles as global carbon sinks. The vast majority of wetland carbon estimates however, has provided only site-specific findings based on small-scale field experiments and have been dependent on specific methods that were used to quantify biomass (Bridgham *et al*. 2006). However, the increased heterogeneity and large spatial gradients within salt marshes and the remarkable temporal variations in salt marsh biomass accumulation rates hinder our ability to draw generalizations based on these local scale site-specific findings (Chapin *et al*. 2006; Davidson and Finlayson 2007). Still, several studies have attempted to draw regional generalizations based on site-specific findings of wetland productivity and biomass (Donato *et al*. 2011) while some other studies provide global to regional scale estimates on salt marsh productivity and carbon accumulation rates using meta-analyses of published data and records (Chmura *et*

al. 2003; Bridgham *et al*. 2006; Komiyama *et al*. 2008, Sahagian and Melack 1998; Kauffman *et al*. 2011). However, Bridgham *et al*. (2006) showed that uncertainty around such estimates to be greater than 100%, mainly due to the greater dependency of carbon estimates on the methods applied. This situation therefore demands methodological approaches to be used in quantitative assessments of salt marsh vegetation characteristics, biomass production and carbon accumulation rates. Further, these methods should be applicable at different spatial scales as well as over different time periods to enable comparisons across space and time, and also to make accurate generalizations over larger spatial and temporal scales.

On the other hand, field-based techniques are labor and time intensive. Further, the inherent heterogeneity and difficulty for direct access of these coastal salt marshes limit the applicability of field estimates for studies at larger spatial and temporal scales. The increasing availability of remote sensing data and techniques over the recent past provides rapid and non-destructive approaches for quantitative assessment of vegetation structural properties, biomass, and thus their carbon dynamics.

In this context, it is important to understand the capabilities of innovative methodological approaches that can integrate field estimates with the remote sensing data and techniques to be used in these less accessible and highly heterogeneous and dynamic salt marsh environments. Such approaches, once developed, could be verified for their accuracies over different areas and at varying spatial and temporal scales. These approaches will then be applicable at regional to global scales and over different

time periods, and therefore will be capable of capturing both spatial and temporal dynamics of these carbon stocks.

The buried carbon in the sediments of intertidal wetlands, including salt marshes, which is often referred to as "blue carbon," is also recognized as a significant carbon sink. Previous studies indicated that wetland soils are sequestering nearly 4.8–87.2 Tg C per year globally (Chmura *et al*. 2003; Duarte *et al*. 2005; McLeod *et al*. 2011). Thus, for a proper understanding and quantification of carbon in the salt marshes, the patterns in the below-ground carbon distribution must also be considered together with the above-ground parts for at least two important reasons. First, a number of studies on *Spartina* spp. indicate that the below-ground biomass and productivity may surpass that of the above-ground parts (Roman & Daiber 1984, Schubauer & Hopkinson 1984, Groenendijk & Vink-Lievaart 1987, Lana *et al*. 1991). Second, the microbial processes in the below-ground environment are closely linked to the functioning of the marsh vegetation (Howarth 1993; Reddy *et al*. 1998, Mendelssohn *et al*. 1981; Lindau & DeLaune 1991).

Within this context, using data from a *Spartina alterniflora* -dominated salt marsh in Galveston Texas, this study evaluates the capabilities of integrating remote sensing data (multi-spectra and lidar) with field measurements for the quantification of carbon pools in salt marsh ecosystems. The first part of this dissertation (Chapter 2) presents a new methodological approach using lidar and multispectral remote sensing data to evaluate their capabilities to provide accurate estimates on salt marsh terrain, vegetation height, cover, and above-ground biomass and carbon quantities. The later

part (Chapter 3) focuses on the spatial patterns in distribution of *Spartina alterniflora* vegetation characteristics and above-and below-ground carbon quantities. Further, the linkages between the temporal changes in the spatial distribution of salt marsh vegetation observed in remote sensing images and the patterns of changes in sediment characteristics along different depths of the soil profile were also evaluated.

The overall objective of this study was to evaluate the increased capability of integrating remote sensing data and techniques with field measurements for quantifying salt marsh carbon stocks. The findings of this study contribute to carbon quantification efforts in these vulnerable ecosystems. Findings of this study will also enhance the understanding of the capabilities of remote sensing datasets and techniques for the quantification of these important carbon stocks.

2. SALT MARSH TERRAIN AND VEGETATION CHARACTERISTICS, AND ABOVE-GROUND BIOMASS ESTIMATES: A DATA FUSION APPROACH USING LIDAR AND MULTISPECTRAL REMOTE SENSING DATA*

2.1 Overview

Herbaceous salt marshes are among the most productive ecosystems on earth. Unfortunately, quantification of the above-ground portion of biomass using passive optical remote sensing is constrained by the complexities of mixed spectral appearance in the water-land environment. Lidar remote sensing, on the other hand has been extensively used to estimate forest biomass, and a few studies have reported their use in characterizing short or herbaceous plants. However, no empirical studies have demonstrated the combined use of lidar and spectral data to quantify above-ground biomass in herbaceous environments, including salt marshes. Thus, the findings of this study will contribute substantially to the understanding of potentials and limitations of using lidar and multispectral data for vegetation characterization and biomass estimates in salt marshes and other similar herbaceous environments. This study, evaluated the increased capability of a data fusion approach using small footprint discrete return lidar and multispectral data to quantify above-ground biomass and thus, carbon stocks in salt marshes. The specific objectives of this study were to: 1) understand the interaction

---

* Reprinted with permission from "Fusion of lidar and multispectral data to quantify salt marsh carbon stocks" by Kulawardhana, R. W., Feagin, R.A and Popescu, S. C., 2013. Remote Sensing of Environment (Special Issue on Remote Sensing of Vegetation Structure, Condition, and Function). Copyright 2013 from Elsevier.

between discrete-return airborne lidar data and marsh vegetation characteristics; 2) determine the appropriate grid size/s of lidar-derived datasets for characterizing salt marsh terrain and vegetation; 3) investigate the applicability of a number of lidar metrics to predict salt marsh vegetation height and above-ground biomass; and 4) to evaluate the utility of integrating multispectral imagery with lidar to improve the predictability of the regression models for quantifying salt marsh above-ground biomass and carbon.

Our results showed that lidar derived Digital Terrain Models (DTMs) in a grid spacing of 5mx5m, provided the best accuracy in terrain elevation estimates with an RMSE of less than 10cm. Regardless of the metrics used, lidar-measured heights underestimated field vegetation heights, which is consistent with the findings of previous studies in short or herbaceous vegetation. The fusion of lidar with multispectral data improved model predictions of live, dead, and total biomass quantities. The improvement provided by the fusion over the use of lidar or multispectral data alone was marginal. However, the best biomass prediction models reported considerably low errors. For example, % RSE for the biomass prediction model using lidar-derived maximum vegetation height (Lmax) was closer to 20%, which is the recommended error threshold for remote sensing based forest biomass prediction models that can be repeatedly applicable for estimating forest carbon stock change. Thus, the findings of this study demonstrate that lidar as compared to spectral data can provide better estimates of above-ground biomass and carbon, even in the herbaceous and low-relief context of a salt marsh.

2.2 Introduction

Recent climate change projections have increased scientific and public attention on carbon cycling and the sequestration of carbon by specific ecosystems. Coastal wetlands, including salt marshes, cover less than 1% of the Earth surface (Duarte *et al*. 2005; Nellemann *et al.* 2009), yet comprise approximately 25% of the global soil carbon sink (Chmura *et al*. 2003). Salt marshes are among the most productive ecosystems on earth (Castillo *et al*. 2010) and play an important role in global carbon cycle (Dixon 1995). In general, their rates of carbon sequestration are an order of magnitude higher than that of comparably-sized rainforests (Bridgham *et al*. 2006; McLeod *et al*. 2011; Nellemann *et al.* 2009). However, these rates vary considerably, both spatially and temporarily. In their extensive review on salt marsh biomass, Castillo *et al*. (2010) highlight remarkable variations in salt marsh biomass accumulation rates and thus suggest studies that can capture this variation. Moreover, the rapid decline in the extent and health of these herbaceous wetland ecosystems (Bridgham *et al*. 2006) has created a need for better understanding of their carbon pools and roles in the ecosystem functioning.

Global-scale carbon studies however, have primarily focused on dry land ecosystems that extend over large areas and have not accounted for the many small, scattered carbon-storing ecosystems such as salt marshes (Ajtay 1979; Olson *et al*. 1983). Although the estimates of the carbon in salt marshes exist, the uncertainty around these estimates remain as high as greater than 100%, mainly due to differences in the methods applied (Bridgham *et al*. 2006) and thus lack comparability across time and

space. Field-based techniques for estimating vegetation height, cover, biomass and carbon are labor and time intensive and are not effective at larger scales. Further, the remarkable spatial and temporal variations in salt marsh biomass accumulation rates hinder our ability to draw generalizations based on local scale, site-specific findings. In contrast, the increasing availability of remote sensing data and techniques provides rapid and non-destructive approaches for quantitative assessment of vegetation structural properties, biomass, and thus their carbon dynamics. More importantly, these approaches are applicable at regional to global scales and over different time scales, and therefore capable of capturing both spatial and temporal dynamics of these carbon stocks.

Recent developments in laser scanning altimetry (also known as lidar – Light Detection and Ranging) have made it an important new data source for the study of 3-D structure of surfaces at sub-meter precision (Baltsavias 1999; MacMillan *et al*. 2003; Rango *et al*. 2000). Unlike satellite-based remote sensing, lidar missions can be flown at almost any time and in most weather conditions providing spatially and temporally continuous datasets. Their laser penetration characteristics present advantages over high resolution passive optical remote sensing data, particularly for the vertical characterization of vegetation (Lefsky *et al*. 2002). Lidar remote sensing has been intensively researched in forestry for estimating tree heights and correlations have been established between field-measured and lidar-estimated tree heights that explain 64% to 99% of the variance in tree heights (Straatsma & Middelkoop 2006). Parameters related to forest density, such as stem number (Lefsky *et al*. 1999; Næsset and Bjerknes 2001),

stem diameter (Drake *et al*. 2002 ; Næsset 2002), timber volume (Nilsson 1996) or basal area (Means *et al*. 1999) have also been predicted (r^2=0.42–0.93) using different lidar variables. Further, these lidar-derived variables relating to vegetation structural properties have been used extensively in biomass predictions of woody vegetation (Boudreau *et al*. 2008; Lefsky *et al*. 2005; Popescu *et al*. 2011), including mangroves (Simard *et al*. 2008). Lefsky *et al*. (2002) and Lim *et al*. (2003) provide reviews on airborne laser scanning of forests, while Zolkos *et al*. (2013) provide a meta-analysis of more than 70 papers on remote sensing of terrestrial above-ground biomass estimates with specific attention to the use of lidar in forest biomass estimates.

Compared to the extensive use of lidar in forestry, little progress has been reported in their applications in vegetation characterization of relatively short herbaceous vegetation. The limited use of lidar in these environments could be attributed to two main reasons. First, dense vegetation with higher canopy closure limits laser penetration to the ground, making estimates of terrain and thus vegetation height challenging and less accurate (Chassereau *et al*. 2011; Hopkinson *et al*. 2005). Second, relatively short vegetation and low variation in vegetation height and canopy characteristics demand data with high accuracy and detailed information content for achieving greater levels of relative accuracies in predicting vegetation characteristics (Rosso *et al*. 2006; Wang *et al*. 2007). Regardless of these limitations, promising results have been reported for estimating terrain as well as vegetation height and cover related variables of relatively short plants using lidar. For example, ground height biases of up to 20 cm have been observed for wetland and riparian vegetation cover (Bowen and

Waltermire 2002; Töyrä *et al*. 2003); vegetation height estimates derived using waveform lidar data have been shown to agree well with field measurements over relatively arid grass and shrub land areas (Ritchie *et al*. 1996; Weltz *et al*. 1994); and other studies have predicted heights of relatively short vegetation in croplands (Davenport *et al*. 2000), grass- and shrub-dominant river floodplains (Cobby *et al*. 2001; Hopkinson *et al*. 2005; Hopkinson *et al*. 2004; Straatsma and Middelkoop 2007), and sagebrush-dominant rangelands (Sankey and Bond 2010; Streutker and Glenn 2006). However, these studies do not agree on a single laser-derived statistic to predict vegetation height or cover. For example, Davenport *et al*. (2000) used the standard deviation within a local window as the predictor of vegetation height for agricultural crops, while Cobby *et al*. (2001) and Hopkinson *et al*. (2004) used it for aquatic grass and shrubs. Moreover, regression equations established in these studies varied greatly; Cobby *et al*. (2001) used a log-linear regression, which did not provide satisfactory results on the data of Hopkinson *et al*. (2004); the slope of the regression equation of Hopkinson *et al*. (2004) was three times higher than the one from Davenport *et al*. (2000). In a different study, Asselman (2002) suggests using the median value of lidar height distribution in a specified local window as the predictor of vegetation height for herbaceous vegetation. Hopkinson *et al*. (2005) followed a different approach to investigate a universal lidar canopy height indicator for different vegetation types with average heights ranging from less than 1m to 24m. Their findings showed that a measure of the grid-based maximum lidar height (Lmax), although potentially better than the standard deviation, varied with laser pulse density and crown morphology.

Therefore, they concluded that this measure cannot be applied universally with the same expectation of accuracy. Based on these findings, it is evident that under specific environments, different vegetation types demand specific methods. More importantly in salt marsh environments, except for a few studies that have used lidar data to characterize terrain variability (Chassereau *et al*. 2011; Collin *et al*. 2010; Montane and Torres 2006; Schmid *et al*. 2011; Yang 2005), there is no literature demonstrating the use of lidar data for quantifying salt marsh cover, density or biomass.

On the other hand, satellite remote sensing has been extensively used in wetland research. Ozesmi and Bauer (2002) provide a comprehensive review on satellite remote sensing of wetlands. Based on their review of more than 100 papers, they state that coastal tidal marshes are the types of wetlands that have been most frequently studied using satellite remote sensing. The majority of these applications are, however on wetland mapping and characterization (Belluco *et al*. 2006; Islam *et al*. 2008; Kulawardhana *et al*. 2007; Wang *et al*. 2007). Some other studies (Hardisky *et al*. 1984; Jensen *et al*. 1998) relate information from spectral data to plant biomass. Similar to lidar data, these methods also suffer from several limitations. First, their signatures are highly affected by atmospheric and background conditions. Second, as the passive optical sensors utilize electromagnetic energy that is reflected or absorbed in the uppermost canopy layers, they are typically less sensitive to vegetation structure (Steininger 2000). In contrast, lidar data, apart from their ability to directly relate to structural characteristics of the vegetation, are not sensitive to vegetation health, condition, or plant productivity (Lefsky *et al*. 2002). Accordingly, several other studies

have applied a data fusion approach by combining lidar and multispectral signatures to predict vegetation biomass in forest environments (Nelson *et al*. 2009; Popescu and Wynne 2004).

Given this background, we hypothesize that a data fusion approach that uses these two types of data (lidar and multispectral) will provide an increased capability for the prediction of vegetation biomass, particularly in herbaceous environments such as salt marshes. Except for a few studies that have combined lidar and multispectral remote sensing for mapping the landscape (Chust *et al*. 2008) or characterization of salt marsh cover (Pavri *et al*. 2011; Rosso *et al*. 2006), we are unaware of any empirical assessment that evaluated such a data fusion approach for quantifying vegetation height in salt marshes. Further, no empirical study has reported the integration of lidar with multispectral data for quantifying biomass of herbaceous vegetation. This study therefore serves as one of the first attempts to evaluate a data fusion approach using lidar and multispectral remote sensing data for quantitative assessment of coastal salt marsh vegetation structure and biomass. Further, the findings of this study will contribute substantially to the understanding of potentials and limitations of lidar and multispectral data for vegetation characterization and biomass estimates in salt marshes and other herbaceous environments.

The primary goal of this study was to evaluate the increased capability of a data fusion approach using small footprint discrete return lidar and multispectral data to quantify carbon stocks in salt marshes. We focus on the estimation of above-ground biomass because it is related closely to above-ground carbon storage. Our specific

objectives were to: 1) understand the interaction between discrete-return airborne lidar data and marsh vegetation characteristics; 2) determine the appropriate grid size/s of lidar-derived datasets for characterizing salt marsh terrain and vegetation; 3) investigate the applicability of a number of lidar metrics to predict salt marsh vegetation height and above-ground biomass; and 4) to evaluate the utility of integrating multispectral imagery with lidar to improve the predictability of the regression models for quantifying salt marsh above-ground biomass and carbon.

2.3 Methods

2.3.1 Study area

Tidal salt marshes along several kilometers of shoreline in West Galveston Bay on Galveston Island, Texas, USA were selected for this study (approximately 10km^2 extent). The study area mainly included the Galveston Island State Park area (Figure 2-1). The marshes were dominated by mono-specific stands of *Spartina alterniflora*, commonly known as smooth cord grass. It is one of the most abundant salt marsh-dominant species in the intertidal zone along the coast of the northern Gulf of Mexico and the Atlantic Coast of North America.

2.3.2 Data

2.3.2.1 Lidar data

Lidar data were acquired in August 2006 by the Sanborn Mapping Company, Colorado Springs, Colorado, using a Leica ALS50 Phase II laser mounted on an aircraft

flying at 900m height with approximately 50% flight-line overlap. The ALS50 II is a discrete return system that measures up to four laser returns per pulse. However, pulse return numbers were not coded into our dataset. Average laser point density and footprint size were 1.4 points per m^2 and 20cm, respectively. The study area spanned three post-processed lidar data tiles. The dataset was available in LAS format and recorded x, y, z and intensity information. The vendor performed a GPS validation survey concurrent to lidar data acquisition and reported absolute accuracies of less than 100cm and 8cm in horizontal and vertical directions, respectively. In this study we did not attempt to characterize the absolute accuracy of lidar data, but instead the relative accuracy between different sample and ground reference points.

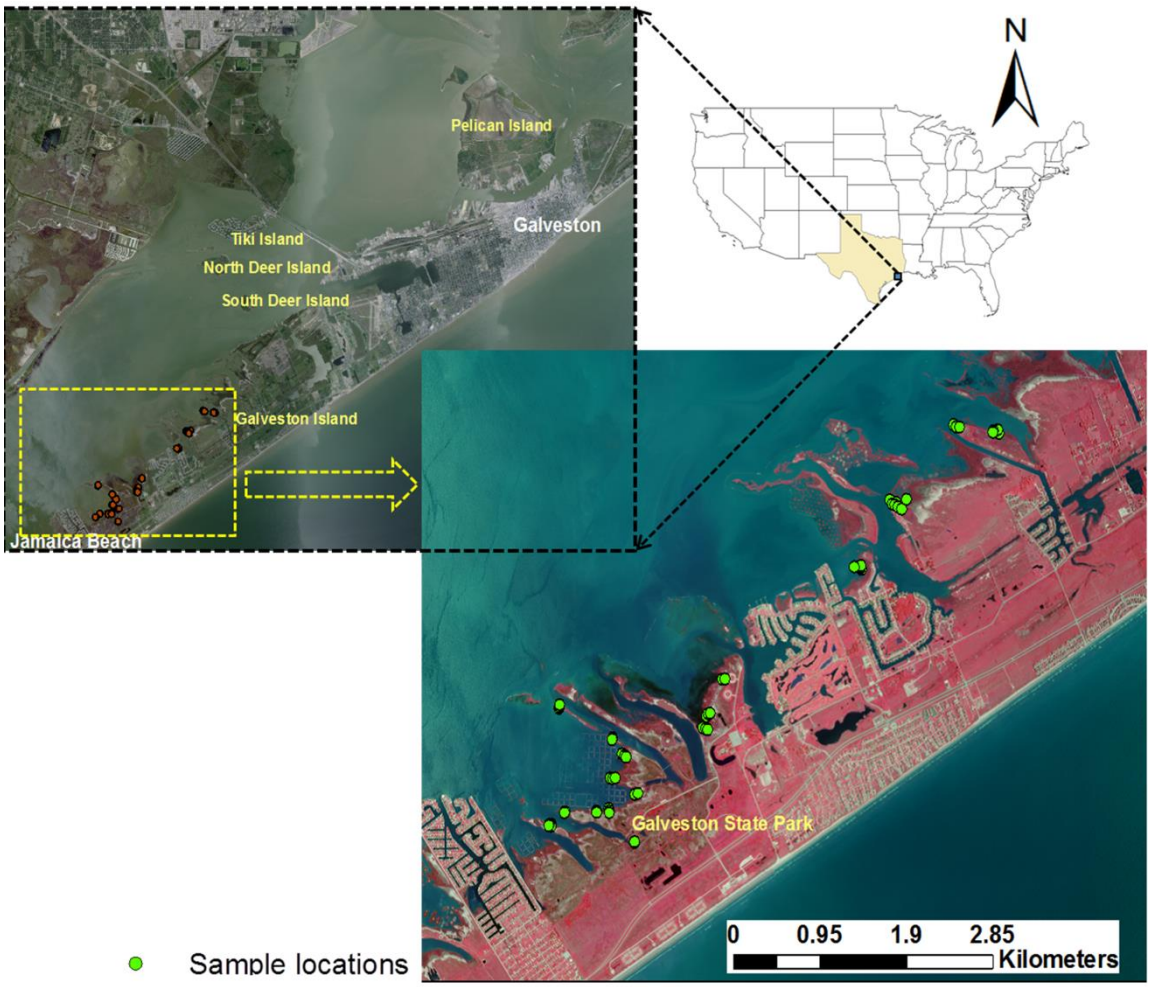

Figure 2-1. Map of the study area. Sample locations are displayed on high resolution aerial imagery acquired in June 2012, displayed using true (upper left) and false (lower right) color composites of red, green, blue and near-infrared bands

2.3.2.2 Spectral data

High resolution (0.5m) digital aerial images were obtained for August 2006 and June 2012 from the National Agricultural Imagery Program (NAIP). These images consists of four (4) spectral bands in blue (428-492 nm), green (533-587 nm), red (608-662 nm), and near-infrared (833-887 nm) regions of the electromagnetic spectrum. Two datasets were required due to the time difference between data acquisitions (lidar, spectral, and field data).

2.3.2.3 Field measurements of vegetation

Castillo *et al*. (2010) propose random sampling as an appropriate sampling method for extensive and mature salt marsh communities where no clumps can be distinguished clearly. In this study, we employed systematic random sampling to incorporate possible vegetation height and biomass variations resulting from environmental and elevation gradients across the study area. Nineteen transects extending from water lines to uplands were established randomly across the study area (Figure 2-1). Spacing between transects varied depending on the spatial distribution of the *Spartina alterniflora* over the study area. However, the average spacing between transects were maintained within the range from 50m to 100m. For the collection of vegetation height, cover, and biomass measurements, 3- 7 sample plots of 3mx3m area were located along each transect. To capture both elevation gradient as well as the heterogeneity in vegetation height and cover, we located these sample plots systematically along transects. Homogeneous plots were selected to minimize sampling bias due to vegetation heterogeneity. This was important given the scale at which lidar

and spectral data were processed and analyzed to correspond with the field measurements. A total of 49 plots were sampled for vegetation height, density, and biomass.

Vegetation heights were measured using two methods. First, the vegetation heights of each 1mx1m grid within 3mx3m plots were visually approximated and measured with a measuring staff (using a graduated measuring stick placed perpendicular to the ground surface, measuring error up to 1cm). Second, all plants within the central grid of 1mx1m were clipped at the ground surface and heights of individual plants were measured in the lab. These measurements were used to derive statistics relating to plot level field vegetation heights and density. We located the sample plots over areas of homogeneous vegetation height and cover conditions and did not clip all the plants at 3mx3m grids to make the field work more efficient. Thus, we assumed that the mean vegetation heights of clipped plants of 1mx1m central grid as a good representation of the vegetation heights of 3mx3m area around the central grid. We verified this using a mean comparison ($p=0.05$) of visually approximated vegetation heights of the two grid sizes.

Clipped plants were processed and analyzed for vegetation biomass (g dry weight per m^2) and carbon estimates, separately for live plants and dead plant material. The most frequent plot sizes reported for salt marsh biomass studies range from quadrats of 0.01 to 0.25m^2 (Castillo *et al*. 2010). The relatively larger quadrat size (1mx1m) was selected in this study to minimize sampling bias and also due to the difficulty of locating individual lidar points and spectral signatures precisely on the ground.

The central coordinates of sample plots and a total of 42 reference points were established using a survey-grade, Global Navigation Satellite System (GNSS) Trimble R2 unit; the Real Time Kinematic (RTK) with infill surveying approach was used, with all points yielding errors less than 4cm horizontal and vertical. All sampled locations were vertically referenced within NAVD 88 units. Reference points (RPs) were located primarily on salt pans and other open and distinguishable areas just outside the Spartina extent, and at road intersections. At each point x, y, and z coordinates were recorded. RPs at road intersections were used to verify locational accuracies of lidar and spectral data, while elevation readings for points within the salt marshes were used to evaluate elevation accuracies extracted from salt marsh DTMs.

Field sampling was conducted from June 4 - 8, 2012. This time of the year was selected to match with the seasonal timing of lidar and spectral data acquisitions. *Spartina alterniflora* is perennial, but shows higher biomass accumulation towards the end of the growing season (Hardisky *et al*. 1984). Castillo *et al*. (2010) suggest recording biomass accumulation at the end of the growing season as a good method to enable comparisons among different studies.

2.3.3 Data processing and analysis

2.3.3.1 Developing Digital Terrain Models (DTMs) using lidar data

The first step in the estimation of vegetation heights using lidar data is the construction of DTMs to enable calculation of laser height distribution relative to the ground surface. However, the accuracy of the derived DTM is determined by our ability

to distinguish between vegetation and ground signals as recorded in lidar data. Previous studies in herbaceous vegetation (Töyrä *et al*. 2003), as well as in forestry (for example, Harding *et al*. 2001; Magnussen and Boudewyn 1998) largely used first and last returns for representing vegetation and ground signals, respectively. Several studies (Næsset 1997; Streutker and Glenn 2006) have used only one of these returns and distinguished between ground and vegetation signals using different approaches, while some other studies have applied filtering approaches on all the pulses using different window sizes (Sankey and Bond 2010). To obtain an accurate representation of the terrain as well as of vegetation surfaces, the methods applied have to be determined based on the characteristics of vegetation, terrain, as well as the data. These characteristics include vegetation cover, the amount of canopy openings, canopy shape, terrain slope, point density of laser pulses, and the reset time of the sensor. For example, lidar has a known sensor limitation for separating returns which are too close in time. This is governed by the reset time of the sensor. For most systems this is around 8-10 nano seconds and translate to a range separation of 1.2 to 1.5m between the recorded returns of the same pulse (Popescu 2011). As a result, when the ground is covered by short vegetation, the laser pulse may provide a return from the canopy top and may even penetrate to the ground surface to generate a ground echo. However, depending on the reset time of the sensor, the last echo may not record as a separate return. This sensor design limitation may contribute to increased errors in terrain as well as vegetation height estimates, particularly if the laser point density is low, and if derived based on first and last returns, respectively. Because of the limitations with one or more of these factors, several other

studies have applied different methods in deriving DTMs using lidar data, particularly for short vegetation. For example, Asselman (2002) suggests using a local minimum within a specified window as representative of the ground surface under relatively open grassland.

Although the salt marshes are known to have dense vegetation cover, in the lower elevations of the *Spartina alterniflora* marshes (areas closer to the water surfaces) where relatively taller plants exist, the ground surface is visible from a vertical perspective. Thus, laser pulses have a greater possibility to penetrate to the ground surface. In contrast, higher elevations of the marshes (the areas away from water surfaces) are characterized by relatively shorter plants and have comparatively higher amount of dead plant material, which can limit laser penetration to the ground surface. However, this dead plant material was primarily located on the ground surface, thus any laser pulse that returned after intercepting this material should closely represent the terrain itself. Considering these vegetation and terrain characteristics, in this study we assumed that some fraction of the returned pulses was reflected from the ground. As such, the lowest point within a specified window was assumed to have fully penetrated the canopy and reached the ground surface, while anything above the minimum was due to vegetation. Thus, we filtered the lowest elevation value of a specified window and applied adaptive triangulation interpolation on these local minima for deriving salt marsh DTMs at different grid sizes. To decide the appropriate window size that best captured the true ground returns, the accuracies of derived DTMs of different grid sizes (3m, 5m,

7m, and 10m) were evaluated by comparing lidar-derived elevations with ground survey elevations. Lidar data were processed using Quick Terrain Modeler (QTM version 7.5).

Our reference points distributed over the study extent (in salt pans and open areas) showed a good match with the derived DTMs and aerial images. Since our focus here is on the salt marsh DTMs, in our accuracy assessment, we used only the points that were inside the salt marsh extent (not including the RPs located outside the *Spartina alterniflora* extent). Further, to evaluate the relative accuracy of lidar data in the vertical dimension, we also calculated Root Mean Square Errors (RMSEs) for each interpolated DTM using ground elevation readings obtained for the RPs established on salt pans and other open areas just outside the *Spartina alterniflora* extent.

2.3.3.2 Lidar metrics as predictors of vegetation height and biomass

After determining the most appropriate grid size, the derived DTM was used as the ground reference for calculating vegetation heights using lidar data. The lidar point heights were then topographically detrended by subtracting corresponding heights of the interpolated DTM from all laser pulse returns. This procedure removed the influence of topography and resulted in laser pulse heights that were now measured relative to ground height; i.e., the same reference plane as the field measured vegetation height data. We assume that there is some interpolation error in the final DTM, commonly less than 10cm (Hodgson *et al*. 2003; Töyrä *et al*. 2003), though this should not bias the vertical laser pulse distributions other than by the potential introduction of a few negative height values, which we assume to have negligible influence on resulting vegetation heights.

A spatial buffer of 3m around the central coordinates of each plot (as recorded in survey-grade GNSS readings) was used to extract the corresponding vegetation heights. Negative heights were observed in a few plots, but the number of negative heights did not exceed two per plot. Assuming these negative values are due to errors in the DTM that are introduced by interpolation and/ or spatial mismatch between lidar and ground GNSS readings, we corrected these negative heights to represent ground surface (h=0). However, in deriving lidar metrics (listed in Table 2-1), we included these zero-height points so as to be characteristic of the data in its entirety.

Evans *et al*. (2009) propose a wide range of lidar metrics for vegetation modeling while several studies reported using different lidar metrics to characterize vegetation heights of short plants. After a thorough review of empirical studies on lidar use for vegetation modeling both in forestry and short and/ or herbaceous vegetation, in this study we evaluated a wide range of lidar metrics (Table 2-1) to be related to vegetation height and biomass in regression models. These include both vegetation height metrics and laser penetration indices. However, only the results for the best indices are discussed in this dissertation.

2.3.3.3 Vegetation indices from spectral data

Over the past decades, vegetation indices (VIs) derived from multispectral bands of remotely sensed imagery have been extensively used in vegetation studies. Among them, normalized difference vegetation index – NDVI (Rouse *et al*. 1973) has been the most extensively used VI in remotely sensed estimates of vegetation biophysical parameters, including biomass in wetland ecosystems (Hardisky *et al*. 1986). However,

several other indices were later proposed to incorporate a soil adjustment factor and/or a blue band for atmospheric normalization. In this study, using the 2006 dataset, we derived a number of VIs (Table 2-1) to relate them with vegetation biomass measurements. In addition, NDVIs derived for two datasets (2006 & 2012) were used in paired t-test (p=0.05) to verify resemblances between two different time periods during which we acquired field and remotely sensed data (lidar and spectral).

2.3.4 Statistical analyses

Mean errors (RMSEs) of salt marsh DTMs derived using different grid sizes were used to evaluate their ability to provide a fit to the true ground surface. Correlations between lidar metrics and vegetation height measurements were first evaluated using Pearson correlation coefficients (r) and scatter plot matrices. To examine the strength of fit between lidar metrics and vegetation heights, simple linear regression analyses were performed using selected lidar metrics as explanatory variables in the model. This selection was based on Pearson r values.

Table 2-1. Summary of plot level lidar metrics and spectral vegetation indices that were investigated as the explanatory variables for estimating vegetation height and biomass.

Metric/ index name	References
Vegetation height metrics	
1. Lmin - Minimum of lidar heights*	Asselman 2002; Ritchie *et al*. 1996; Weltz *et al*. 1994 – to estimate terrain in grasslands
2. Lmax – Maximum of lidar heights*	Ritchie *et al*. 1996 - for arid grasslands; Rango *et al*. 2000 - for Coppice dune characterization
3. Lmean– Average of lidar heights*	Hopkinson *et al*. 2004; 2005 – For mixed vegetation
4. Lmode– Mode of lidar heights*	Not reported
5. LSD– Standard deviation of lidar heights *	Davenport *et al*. 2000; Cobby *et al*. 2001 - for crops and grasses
6. Lvariance– variance of lidar heights*	Not reported
7. Percentiles (L10, L25, L50, L756, L80, L90) - 10^{th}, 25^{th}, 50^{th}, 75^{th}, 80^{th}, 90^{th} percentiles of lidar heights* respectively)	Asselman 2002; Ritchie *et al*. 1996; Weltz *et al*. 1994 - for grasslands, Straatsma and Middelkoop 2007 - for river flood plain vegetation

* *Detrended lidar heights*

Table 2-1. continued.

Metric/ index name	References
Laser penetration indices	
1. LCD-Canopy density (defined as percentage vegetation returns**) $\frac{\#\ of\ non-ground\ (vegetation)\ returns}{\#\ of\ total\ returns} * 100$	Weltz *et al*. 1994, for rangeland vegetation height and canopy cover; Straatsma and Middelkoop 2007 - for river flood plain vegetation
2. Number of non-ground (vegetation) returns**	Not reported
3. Number of total returns**	Not reported
Vegetation Indices	
1. Normalized difference vegetation index – NDVI (Rouse *et al*. 1973) $\frac{(NIR - R)}{(NIR + R)}$	Hardisky *et al*. 1984; 1986 –to predict biomass in Delaware salt marshes; Jensen *et al*. 1998 - to predict biomass and LAI in S. Carolina salt marshes
2. Soil Adjusted Vegetation Index, SAVI (Huete 1988) $\frac{(NIR - R)}{(NIR + R + L)} * (1 + L)$ Introduce a weighting factor to red and near-infrared bands to reduce sensitivity to soil brightness variability	Baptiste and Jensen 2006 – to predict mangrove biophysical parameters; Jensen *et al*. 1998 - to predict biomass and LAI in Spartina salt marshes.

***Different height bins were evaluated to define ground height as recorded in detrended lidar data*.

Table 2-1 continued.

Metric/ index name	References
1. Modified Soil Adjusted Vegetation Index, MSAVI (Qi *et al*. 1994a) $\frac{(2NIR+1)-\lceil(2NIR+1)^2-8(NIR-R)\rceil^{0.5}}{2}$ Algebraic solution to an iterative variant of SAVI in which the weighting factor is self-adjusting	Zhao *et al*. 2009 – To characterize estuarine wetland vegetation succession
2. Atmospherically Resistant Vegetation Index, ARVI (Kaufman and TanreÂ 1992) $\frac{(NIR-2R+B)}{(NIR+2R-B)}$ Simple linear combination of blue and red reflectance to compensate for the increase in path radiance with aerosol optical depth	Zhang *et al*. 1997 – To predict salt marsh biomass in San Pablo Bay, California
3. Atmospheric and Soil Vegetation Index, ASVI (Qi *et al*. 1994b) $\frac{(2NIR+1)-\lceil(2NIR+1)^2-8(NIR-2R+B)\rceil^{0.5}}{2}$ Uses a combination of the corrective principles behind ARVI and MSAVI	Jensen *et al*. 1998 - for salt marshes
4. Green vegetation index, VIGreen (Gitelson *et al*. 2002) $\frac{(Green-R)}{(Green+R)}$	Jensen *et al*. 1998 - for salt marshes

Further, to evaluate combinations of lidar metrics that could better predict the vegetation height, multiple regression analyses were performed using all lidar metrics as explanatory variables in the model. The best fit model was selected using Mallow's Cp selection method with Akaike Information Criterion (AIC) as the model fit statistic. The AIC method selects the best fit model by penalizing models with redundant variables (Akaike 1981). This, method also allows the selection of the best fit model while minimizing the problem of multi-collinearity. However, since most of lidar metrics and VIs were highly correlated, variance inflation values (VIFs) reported for each explanatory variable in the model were also examined and retained only the variables with VIFs of less than five (Belsley 1980).

In order to evaluate the applicability of each method (lidar and spectral) for quantifying vegetation biomass, above steps were applied on lidar metrics and VIs separately. In biomass regression models using lidar metrics, in addition to the vegetation height indices, laser penetration indices were used as proxies for vegetation cover and /or stem density. Regression relationships between lidar metrics and above-ground biomass were evaluated, because biomass is related closely to above-ground carbon storage. Relationships between VIs and height measurements were nit evaluated, as it was not the focus in this study. To evaluate the increased capability of a data fusion approach, lidar metrics and VIs were then combined as explanatory variables in multiple regression models. Various transformations of the independent variables (i.e., inverse, log) were also explored in an attempt to improve regression relationships. Model results were also tested for heteroscedasticity. Results did not indicate a necessity for

transforming the dependent variables. The relationships for different biomass components were investigated separately (live, dead, and total biomass).

To enable comparisons of the accuracy of the models in this study with similar studies, RMSE reported for each model were standardized by mean biomass from field measurements (i.e. RSE/mean biomass). We refer this statistic as % RSE, i.e., the RMSE expressed as a percent of mean biomass. Zolkos *et al*. (2013) discuss the advantage of % RSE over RMSE in detail.

Statistical analyses were performed using SAS Enterprise Guide (version 5.1).

2.4 Results

2.4.1 Salt marsh DTMs using lidar data

Accuracies of derived DTMs at different grid sizes are summarized in Table 2-2. RMSEs indicate relative accuracies of each DTM while correlation coefficients (r^2) determine the strength of agreement between ground-measured and lidar-derived elevations at different grid sizes. The effects of vegetation on DTM accuracies can be evaluated by comparing these statistics that are associated with RPs that were located on salt pans and vegetation points separately.

Table 2-2. Accuracies of lidar derived DTMs.

Sample points included in the analysis		DTM grid size (m)			
		3	5	7	10
Sample points (49) located within *Spartina alterniflora* extent	RMSE (m)	0.09	0.10	0.13	0.16
	R^2	0.68	0.73	0.51	0.42
Sample points + salt pans and other open areas outside the *Spartina alterniflora* extent	RMSE (m)	0.08	0.09	0.14	0.21
	R^2	0.80	0.87	0.77	0.65

Notes: Accuracies of salt marsh DTMs were evaluated based on RMSEs calculated using GPS elevations of a total of 61 ground points (sample plots + salt pans) located within the salt marsh extent.

The ability of salt marsh DTMs to predict the surface decreased with increasing grid size, with mean errors ranging from 0.09m to 0.16m (Table 2-2). However, only slight fluctuations in r^2 values were observed when local minima were interpolated using smaller window sizes (3m and 5m). Further, the RMSEs of the salt marsh elevation estimates derived using two grid sizes were not significantly different. As the window size increased further, relatively greater fluctuations in both r^2 and RMSEs were observed. In addition, predicted elevations were consistently lower when the DTMs of larger grid sizes were used (Figure 2-2). This could be largely due to the effect of smoothing. Defining local minima using larger window sizes was found to remove smaller terrain variations that would otherwise increase errors in elevation estimates.

This effect was also evident in salt marsh elevation profiles created using DTMs of different grid sizes (Figure 2-2).

In general, the presence of vegetation is reported to degrade the accuracies of lidar-derived terrain estimates. However, in this study, when DTMs were interpolated using smaller window sizes (3m and 5m), we did not observe significant ($p<0.05$) differences in mean errors between open and vegetated areas (i.e. salt pans and sample plots). However, when using larger window sizes (7m and 9m), mean errors for open areas were significantly ($p<0.05$) higher as compared to vegetated sample plots (Table 2-2) and reflected the increasing levels of interpolation errors, particularly across abrupt changes in surface heights. Thus, in order to minimize the effect of interpolation errors and considering the low point density of lidar data used in this study, the 5m grid size was selected as the most appropriate for deriving salt marsh DTMs. In our study area, *Spartina alterniflora* appears to be distributed over a narrow elevation range from 0 to less than 0.5m.

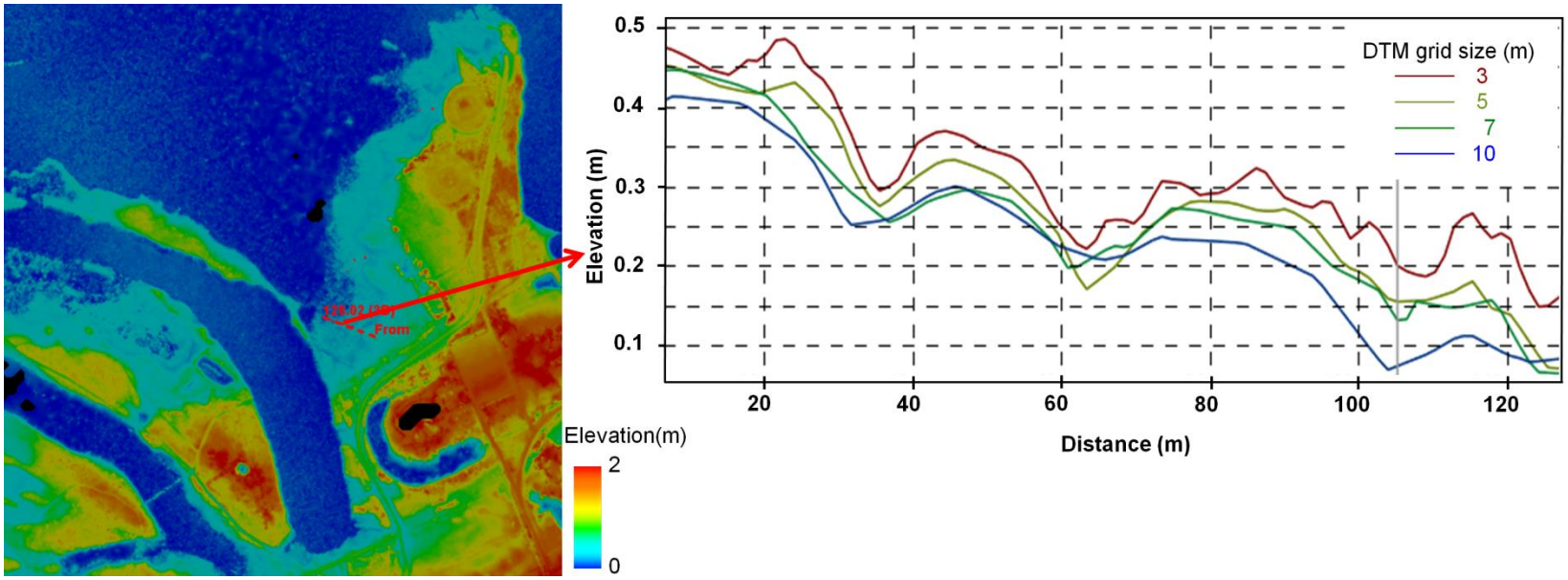

Figure 2-2. An example cross section of the salt marsh showing elevation differences among DTMs of different grid sizes (3m, 5m, 7m, and 10m).

2.4.2 Lidar metrics as predictors of vegetation height

In our study area the mean vegetation height of *Spartina alterniflora*, as measured from the plants clipped within each 1m x 1m plot, was 43.7±6cm. Visually approximated vegetation heights in the field at 1m x 1m and 3m x 3m scales were not significantly different from one another ($p>0.05$). These visual assessments, however, were consistently higher than the averages of clipped plants. This indicates that our visual approximations tend to be biased towards the taller plants inside the canopy, which was also reported by Rosso *et al*. (2006) for *Spartina alterniflora* in San Francisco Bay. However, visually approximated vegetation heights within the 1m x 1m area were highly correlated ($r^2 = 0.92$, $p<0.001$) with the mean heights of clipped plants. Thus, the vegetation height measurements of clipped plants at 1m x 1m plots could be considered as a good representation of the 3m x 3m area, and were related to lidar and spectral data.

Although the regression relationships between lidar estimates and field measurements of vegetation heights were not strong, they were significant ($p<0.001$) for all lidar height metrics. Lmax provided the best agreement with field height measurements and explained 41% of the variance in vegetation heights (RMSE = 5.85cm). This was followed by L90 ($r^2=0.40$, RMSE = 5.94cm), and Lmean ($r^2=0.34$, RMSE = 6.22cm). These lidar metrics however, consistently underestimated the vegetation heights (Figure 2-3). Linear regression analysis between Lmax and vegetation heights determined the best model as: VHfield (vegetation height) = 0.79Lmax + 32cm. This model had the lowest RMSE value at 5.5cm. None of the laser penetration indices reported a significant relationship to vegetation height.

Lidar height metrics showed a high degree of multi-collinearity (Figure 2-4), and when used in multiple regression analyses, they did not improve the predictability considerably. However, multiple regression analysis returned Lmax, Lmean, and LCD (in which the ground level was set to 10cm) as the only significant variables in the model. This model explained 47% of the variance in field measured vegetation heights, while Lmax alone explained 41% of the variance (Figure 2-3).

After evaluating different thresholds and the relative mean errors of the DTMs, the height bin of 10cm was selected as the threshold for defining LCD. The best multiple regression model was: VHfield (vegetation height) = 0.56Lmax + 1.39Lmean+0.20LCD +15.45cm.

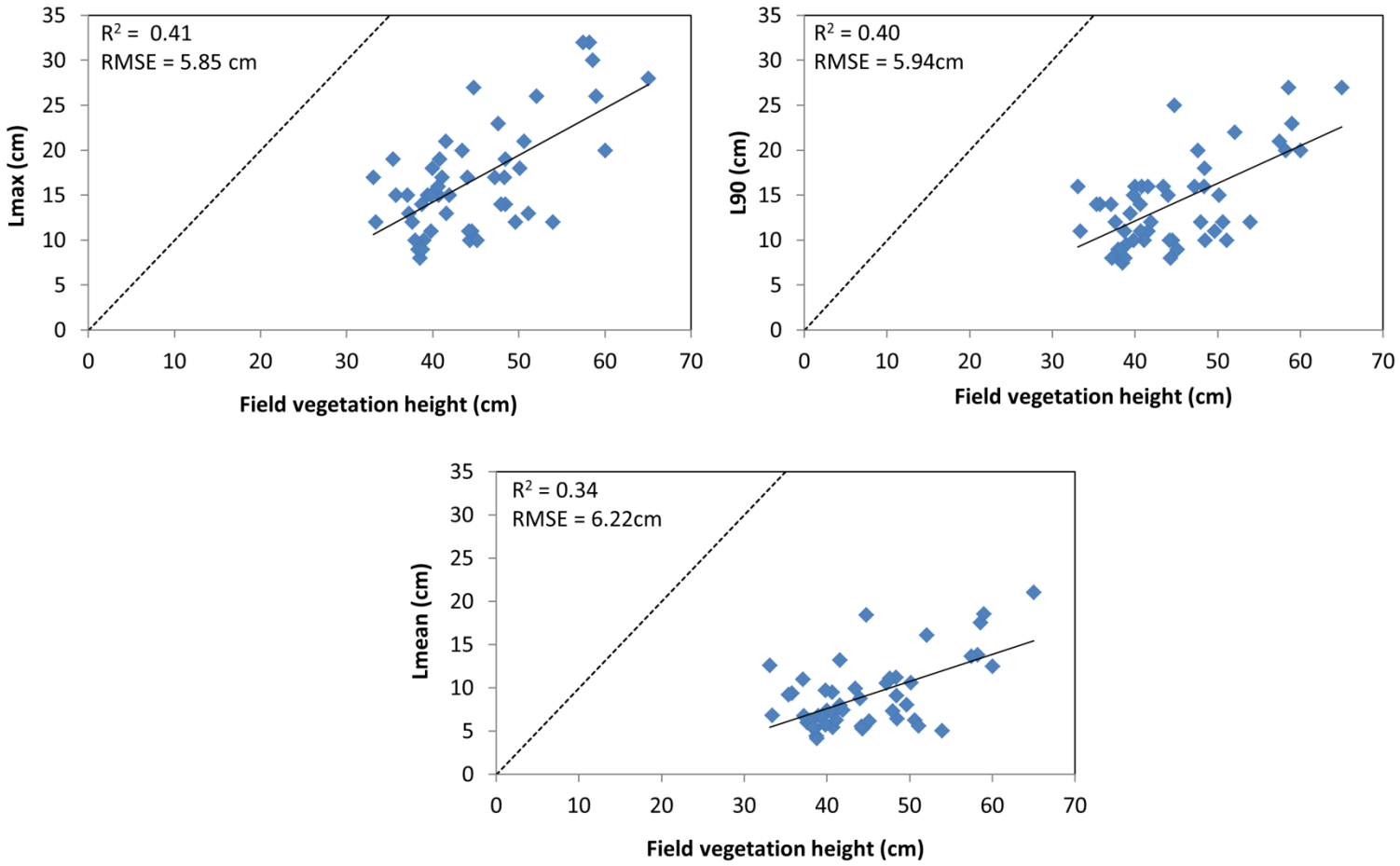

Figure 2-3. Correlations between lidar metrics and field vegetation heights. Solid lines represent the best fit linear regressions while dashed lines are the 1:1 correspondence (perfect fit) between field and lidar-derived vegetation heights.

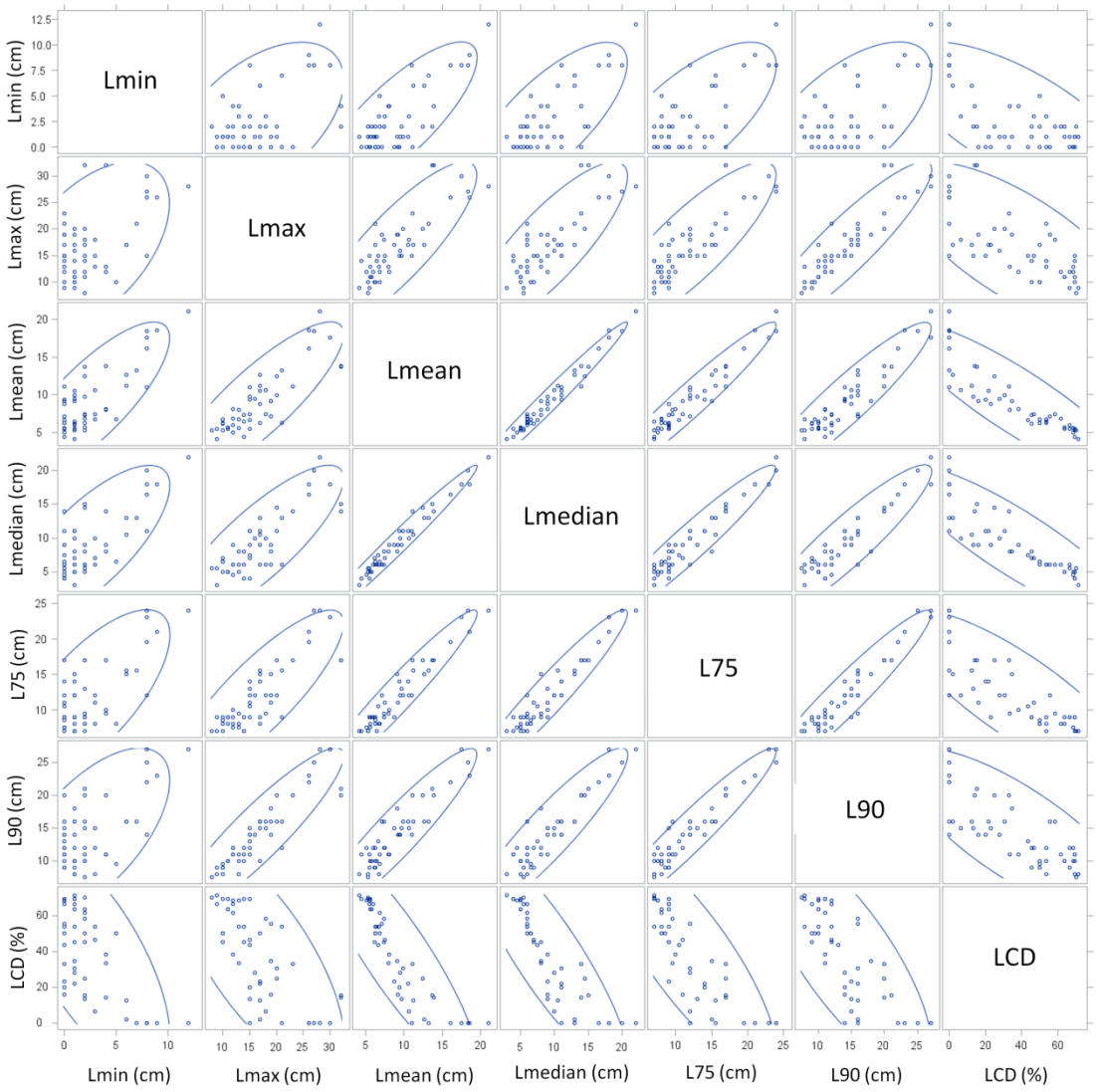

Figure 2-4. Multi-collinearity among the lidar metrics. Scatter plot matrix is shown for the lidar derived variables that are better correlated to field measurements (either height or biomass).

2.4.3 Lidar metrics as predictors of vegetation biomass

Mean above-ground biomass for our study area was 882g per m^2. Live and dead biomass components accounted for 61% and 39% of the total vegetation biomass, respectively. Similar to the vegetation height estimates, lidar height metrics showed a highly significant positive correlation ($p<0.001$) with live vegetation biomass. RMSEs for these models ranged from 103 to 154 g dry weight per m^2, while r^2 values were within the range of 0.10 to 0.37. Lmax reported the highest correlation to live biomass, however it explained only 37% of the variance in the data (Figure 2-5a). The % RSE for this model was closer to 20%, which is the recommended error threshold for remote sensing based forest biomass prediction models that can be repeatedly applicable for estimating forest carbon stock change (Zolkos *et al*. 2013).

None of the metrics were related to dead biomass. Accordingly, as compared with live biomass, consistently lower r^2 values were found for total biomass. The maximum r^2 reported for total biomass was 0.13 and was found using the Lmax metric (Figure 2-5b). As in the case of vegetation height estimates, laser penetration indices did not relate to any of the biomass components. Further, multiple regression models did not improve predictability for any of the biomass components and this could be largely attributed to multi-collinearity among lidar metrics (Figure 2-4).

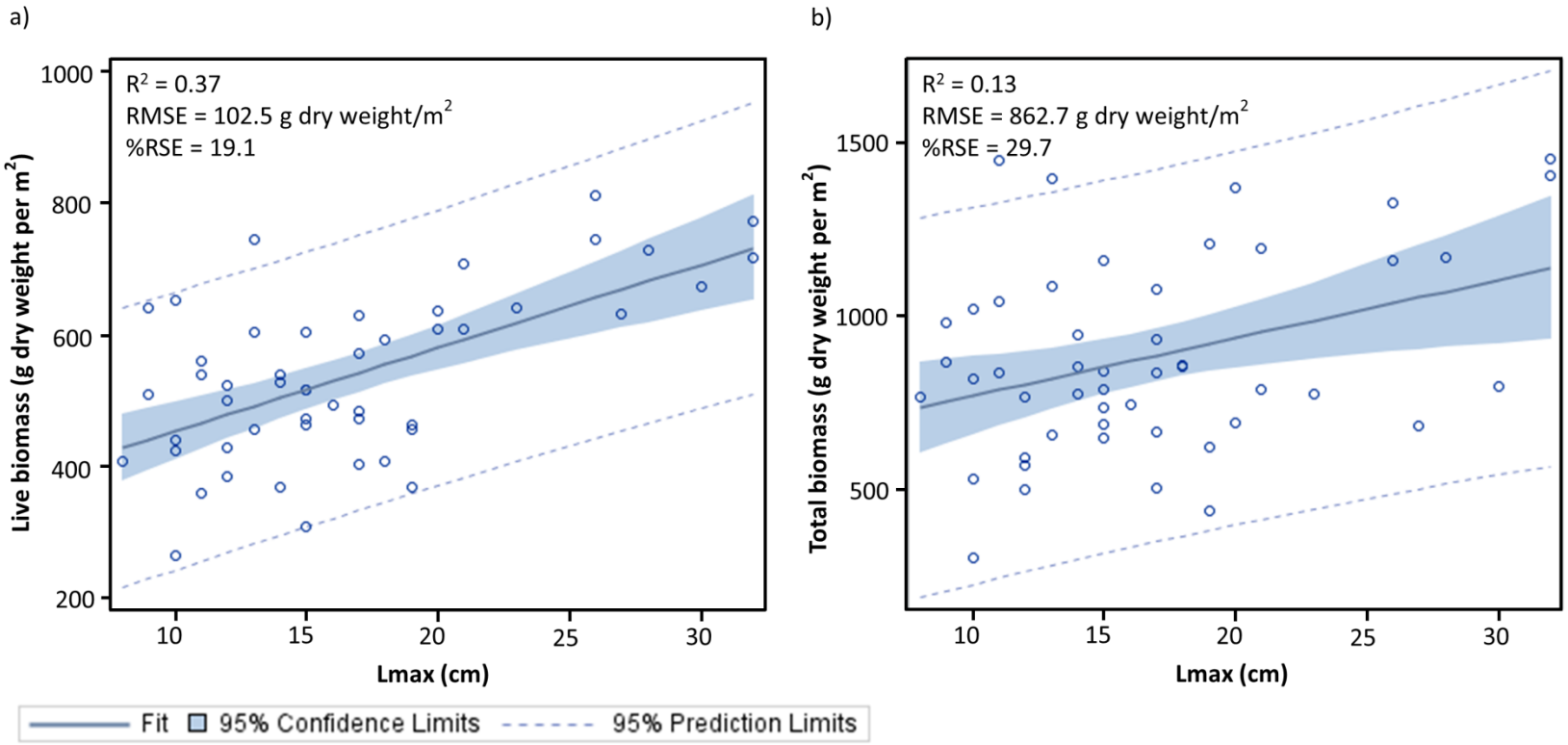

Figure 2-5. Goodness of fit between lidar metrics (Lmax) and vegetation biomass measurements: a) Live biomass, and b) Total biomass.

2.4.4 Vegetation indices as predictors of vegetation biomass

Regression relationships between vegetation indices and live vegetation biomass were also significant (p=0.001). These indices however, explained up to 28% of the variance in live biomass measurements (r^2 values ranged from 0.14 to 0.28). NDVI and SAVI reported to be the best predictors of live biomass (r^2 =0.28). RMSEs for these relationships were similar to that of lidar based live biomass predictions. As reported in previous studies, all vegetation indices were highly correlated (r^2 values ranged from 0.84 to 1) with each other. Except for VIGreen, the others did not show significant correlations to dead or total biomass. VIGreen explained 14%, 15%, and 24% of the variance in live, dead, and total biomass, respectively.

2.4.5 Fusion of lidar and multispectral data for vegetation biomass predictions

As expected, the data fusion approach improved regression models for predicting both live and dead biomass and thus, better predicted total biomass (Table 2-3). However, these improvements were marginal. For example, the combination of lidar and multispectral data explained 47% of variance in live biomass measurements, whereas the best models using lidar and spectral data alone explained 37% and 28% of variance in live biomass measurements, respectively. Similarly, VIGreen explained 15% and 24% of variances in dead and total biomass data, respectively while the combination of lidar metrics improved this only up to 24% and 33%, respectively.

Table 2-3. Results of multiple regression models for predicting vegetation biomass.

	R^2	RMSE (g dry weight/m^2)	% RSE	Best fit model
Live	0.47	86.1	16.0	Live BM = 10.13*Lmax + 638.09*SAVI +179.64
Dead	0.19	200.89	58.3	Dead BM = 4.43 *LCD + 1197.4*VIGreen + 365.05
Total	0.33	229.20	25.9	Total BM = 15.51*Lmax + 5.35*LCD + 1331.7*VIGreen+ 639.13

Note: All relationships were significant at 99% confidence.

2.5 Discussion

This study substantiates similar findings from earlier studies in herbaceous environments that used lidar data for quantifying vegetation height. However, we are not aware of any study that attempted using lidar or a data fusion approach using lidar and spectral data to predict vegetation biomass in herbaceous environments. Thus, we discuss our findings on biomass relationships in comparison with similar studies from forest environments. However in doing so, we pay attention to the differences in vegetation canopy and terrain characteristics between these two contrasting environments.

2.5.1 Accuracies of salt marsh DTMs of different grid sizes

In this study, we first wanted to decide on the appropriate scale for deriving salt marsh DTMs using lidar data. While deriving DTMs, we also wanted to ensure that the lidar returns we used to interpolate DTMs are true ground signals rather than from vegetation. This is important given the salt marsh vegetation structural characteristics. The majority of previous studies in both forest and short or herbaceous vegetation have selected either the first or the last return as the ground signal. Considering the vegetation characteristics of our study area we applied a different approach, which filtered the lowest point within a specified grid size. Our assumption is that a portion of laser pulses penetrate fully through the canopy and return from the ground. This approach has been previously applied in different environments (Schmid *et al*. 2011; Weltz *et al*. 1994; Streutker and Glen 2006). Different studies, however, reported that the accuracy of the lidar estimated elevation to be largely determined by: 1) vegetation

structure such as level of canopy openings, canopy shape, and leaf orientation (Cobby *et al*. 2001; Hodgson and Bresnahan 2004; Hopkinson *et al*. 2004; Nelson 1997); 2) terrain, mainly slope and surface irregularities (Hodgson *et al*. 2003); and 3) sensor characteristics, particularly the laser point density (Straatsma and Middelkoop 2007) and minimum range separation between multiple returns. Considering these factors, we wanted to identify the appropriate window size that best captured true ground returns, while also maintaining terrain irregularities to give a fair representation of the vegetation height variations.

The errors of lidar derived DTMs increased as we increased the window size and reflected the effect of smoothing. Further, the errors, when evaluated separately for points within and outside the vegetation cover, revealed that the bias in DTM elevation is attributed to the interpolation errors rather than the presence of vegetation (Table 2-1). These errors were more prominent when DTMs were interpolated at larger grid sizes (>5m). However, the results of some previous studies reported increasing DTM errors with increasing vegetation cover (Hopkinson *et al*. 2004; Cobby *et al*. 2001). The effect of vegetation on deriving ground elevation is largely determined by the combination of the three factors discussed above and thus, specific to each environment. In this region, Spartina salt marshes reported to reach maximum production, and thus cover, during late summer (Hardisky *et al*. 1984). However, even under these conditions, due to relatively smaller leaf angles and narrow leaf blades of Spartina plants, we can expect a sufficient level of canopy openings to allow ground penetration of laser pulses. Thus, considering terrain as well as vegetation characteristics of the study area, and the low point density

of lidar data used in this study, we selected the 5m grid size as the most appropriate for deriving salt marsh DTMs for our study area.

In this study, when using a window size of <5m relatively smaller errors (<10cm) in the DTMs were observed. These findings are similar to the findings of some previous studies; Wang *et al*. (2007) used a similar approach for filtering ground signals in salt marshes of the lagoon of Venice, Italy and reported an RMSE of 6.4cm, while it was 7cm for low gradient salt marsh in South Carolina (Montane and Torres 2006), and 13cm for San Francisco Bay marshes in California (Rosso *et al*. 2006). However, the latter study reported that none of the lower points within the vegetation appeared to be sufficiently close to the ground, and inferred that new *Spartina alterniflora* growth was too dense for complete penetration of laser pulses. This may remain true even in our study area, particularly for the higher elevations of the *Spartina alterniflora* marsh where relatively dense accumulation of dead plant material was observed. These dead plant materials act as a dense mat and remain close to the ground, thus their contribution to the errors in elevation estimates could be small.

The general concept is that in dense canopies, limited laser penetration to the ground affects the accuracies of derived vegetation estimates (Hopkinson *et al*. 2004; Lefsky *et al*. 2002). However, as in the previous studies mentioned above, our findings reveal that lidar data are capable of accurately estimating salt marsh terrain (RMSE<10cm) if appropriate methods are applied by considering data, vegetation, and terrain characteristics relevant to the area of interest.

2.5.2 Lidar metrics as predictors of vegetation height

While it was not the scope of this study to characterize vegetation height variations across the study area, we attempted to evaluate lidar metrics that better capable of predicting vegetation heights at a given spatial scale. In evaluating this, it is important to understand the spatial unit that better explain variation in both terrain and vegetation. Even though the relative accuracies of derived DTMs at 5m and 3m were not significantly different, given the low elevation gradient, we favored 5m DTM over 3m DTM. However, to account for the vegetation height variation, and also to minimize the discrepancy between the coverage of field measurements and lidar and spectral information, we analyzed lidar and spectral data at 3m spatial resolution.

Lidar height metrics consistently underestimated salt marsh vegetation heights (Figure 2-3). The best model that used the three lidar height metrics (Lmax, Lmean, and LCD) underestimated vegetation heights by an average of 15cm. This underestimation is approximately 30% of the mean vegetation height. Underestimation of canopy height is reported in many lidar studies in forestry (e.g., Magnussen *et al*. 1999; Gaveau and Hill 2003). Similar results were reported in previous studies of herbaceous vegetation as well. For example, Ritchie *et al*. (1996) and Weltz *et al*. (1994) attributed lidar underestimation of rangeland vegetation heights to the errors associated with lidar-derived ground estimates, which they explained using inadequate laser penetration to the ground surface. Struetker and Glenn (2006) explained this using laser returns from below the canopy tops of sagebrush vegetation. Given the salt marsh vegetation characteristics in our study area, the lidar underestimation of vegetation heights in this

study can largely be explained using increased laser pulse penetration into the foliage. Although we assume laser pulses to be returned from the top of the canopy surfaces, even the maximum heights of laser pulses may have returned from inside the canopy. The vegetation characteristics of Spartina, including less dense vegetation cover, smaller leaf angles, and narrow leaf blades may have collectively contributed to the increased penetration of laser pulses through the canopy. Some other studies have indicated lidar underestimation of canopy heights as a result of insufficient representation of canopy apexes due to low sample point density (Hodgson and Bresnahan 2004; Straasma and Middelkoop 2007; Hopkinson *et al*. 2005), which also can be applicable to our study using lidar data of 1.4 points per m^2. Further, some overestimation of ground surfaces due to minimal pulse penetration through dense vegetation (Adams and Chandler 2002; Hodgson and Bresnahan 2004; Weltz *et al*. 1994) and sensor limitations in range separation, and interpolation errors may also have contributed to the vegetation height underestimation. Mean errors in vegetation height estimates reported in this study (RMSEs of less than 7cm) are however comparatively smaller in magnitude as compared to the findings from forestry. Our findings also resemble the findings of some previous studies in herbaceous environments. For example, Davenport *et al*. (2000) and Cobby *et al*. (2001) reported lidar crop height estimates with accuracies of less than 10cm and 14cm, respectively. The increased accuracies in terrain estimates in our study may have largely contributed to relatively smaller errors in vegetation height estimates.

The regression relationships between lidar metrics and vegetation heights, even though highly significant ($p<0.001$), explained only 47% of the variance in vegetation

heights. A few studies in herbaceous vegetation reported stronger relationships (r^2 values ranging from 0.75 to 0.89) between vegetation heights and lidar metrics (Ritchie *et al*. 1996; Davenport *et al*. 2000; Cobby *et al*. 2001; Hopkinson *et al*. 2004). Except for the Ritchie *et al*. (1996) study, vegetation heights in these studies were of a relatively wide range and included comparatively taller plants. Ritchie *et al*. (1996) used laser profile data, thus their relatively higher information content could have contributed to smaller errors and higher r^2 values.

In a study on sagebrush steppe, Struetker and Glenn (2006) used a similar approach for extracting terrain and vegetation heights and reported similar findings (Pearson correlation coefficient, r = 0.72). However, they reported different lidar height metrics as better predictors of vegetation height and suggested surface roughness, which is estimated using standard deviations of detrended lidar heights to be the best predictor of vegetation heights. In contrast, our findings revealed Lmax, which is the maximum of lidar-derived vegetation heights as the best predictor of salt marsh vegetation height when used alone. This corresponds with the findings of Hopkinson *et al*. (2004) that reported Lmax as a better canopy height indicator over homogeneous vegetation. In this study, Lmax was followed by the 90th percentile of lidar-derived vegetation heights (L90). In general, salt marsh vegetation heights follow the elevation gradient; vegetation height generally increases as elevation decreases. Consequently, lower elevations within the *Spartina alterniflora* marsh are characterized by relatively taller plants, while in higher elevations shorter plants exist. Under these conditions, the upper end of the lidar-derived vegetation height distribution (Lmax, L90) was found to better capture this

variation in the vegetation height distribution rather than the variation in vegetation height within a specified area (in this case within a specified grid).

2.5.3 Lidar metrics as predictors of vegetation biomass

A wide collection of lidar metrics have been reported in literature as the predictors of forest biomass. However, no empirical study has reported their applicability for biomass predictions in herbaceous environments. Therefore, we discuss our findings in relation to the findings reported in forestry.

The above-ground biomass quantities of *Spartina alterniflora* reported to be in the range from 100 – 3700 g dry weight per m^2 (Castillo *et al*. 2010). The values reported in our study varied within a narrow range from 304 to 1452 g dry weight per m^2. However, these values are within the average reported for *Spartina alterniflora* salt marshes over the North Gulf coast of US (Hardisky *et al*. 1984). Further, these above-ground biomass levels are low as compared to those reported in forestry. Therefore, we can infer that in addition to data limitations (i.e. low point density of lidar data, temporal mismatch between field and lidar data acquisitions, and scaling issues), the narrow range of vegetation biomass levels reported in this study may also have contributed to lowering the r^2 values in this study.

Early studies in salt marshes have shown strong relationships between plant heights (Hardisky *et al*. 1984; Hardisky *et al*. 1986) and vegetation biomass, while some others reported biomass relationships to vegetation cover (Castillo *et al*. 2008). These studies thus developed empirical relationships based on plant height and vegetation cover parameters for predicting vegetation biomass. In this study we observed highly

significant ($p<0.0001$) and very strong relationship ($r^2 = 0.97$, RMSE = 90g dry weight per m^2, % RSE = 17) between measured plant height and live biomass. In biomass predictions using lidar metrics, we can consider that lidar height metrics and laser penetration indices to serve as proxies of vegetation heights and cover, respectively. This in turn explains the relatively lower r^2 values reported for the relationships of lidar metrics to vegetation biomass as compared to that of vegetation height.

In this study, none of the laser penetration indices were significantly correlated ($p=0.05$) to any of the vegetation cover or biomass measurements. In Spartina salt marshes, stem density can be used as a good indicator of vegetation cover (Castillo *et al*. 2008). In our study area, the average stem density was 356 per m^2. Even though this number is not very high as compared to the numbers reported in other salt marshes (Castillo *et al*. 2008; Hardisky *et al*. 1984), given the low point density of the lidar data we used, we can infer that the amount of information recorded in these lidar data are not sufficient to make inferences on vegetation cover of these salt marshes. This mis-match partly explains the inability of multiple regression models that combined lidar height and laser penetration indices to improve biomass predictions. As in vegetation height predictions, multi-collinearity among lidar metrics also limited the capabilities of multiple regression models to improve biomass predictions.

Regardless of the low r^2 values reported for the relationships between lidar-derived vegetation indices and biomass measurements, the best biomass prediction models reported considerably low RMSEs and % RSEs. Some of the best models reported remarkably low errors when standardized using mean biomass levels. For

example, % RSE for the best model using Lmax was 19.1%. Zolkos *et al*. (2013) recommend an error threshold of <20% RSE for remote sensing based models that can be repeatedly applicable for estimating forest carbon stock change. Hence, we can infer that these models provide promising results for estimating salt marsh vegetation biomass and thus carbon. Further, we are not aware of any empirical study that used lidar data to predict biomass in herbaceous environments. Within this background, we believe that this study will serve as a turning point to increase research attention within this field, particularly to investigate the capabilities of lidar techniques in biomass studies under different environments outside forestry.

2.5.4 Vegetation indices as predictors of vegetation biomass

Although we investigated a wide collection of vegetation indices, our best model explained only 28% of the variance in biomass measurements. Previous studies of similar herbaceous vegetation, but in different environments including rangelands (Waller *et al*. 1981) and agricultural vegetation (Richardson and Everitt 1992), reported stronger relationships (r^2 ranging from 0.7 to <1) between spectral measurements and vegetation biomass. Similarly, in salt marshes, Hardisky *et al*. (1984) reported an r^2 value of 0.79 for relationship between Spartina green biomass and NDVI. However, their spectral measurements were obtained using a hand-held radiometer concurrently with field biomass measurements. Further, their regression models were based on cumulative measurements over an entire growing season.

Hardisky *et al*. (1986) reported that the presence of dead biomass within the canopy influences the spectral signatures by decreasing the reflectance in NIR region

and thus NDVI, and therefore obtained spectral measurements after removing standing dead biomass under the canopy. Further, standing water within the marsh can also affect spectral signatures. For example, as in other salt marshes, in our study area low elevations are characterized by relatively dense clusters of taller plants as compared to the shorter and relatively drier plants that are evenly distributed in higher elevations. Thus, the greener and relatively moist vegetation in low marshes should provide a strong signal in the NIR region as compared to that of high marshes. However, this NIR signal could be largely absorbed even in low marshes particularly due to the presence of water underneath the canopy, whereas in high marshes relatively larger amounts of dry biomass could be influential.

We acquired field and remotely sensed data to match with seasonal changes. NDVIs between two datasets (2006 and 2012) did not reveal significant changes ($p = 0.05$). However, changes in both vegetation height and cover can be expected during different years.

In summary, remarkably low r^2 values between VIs and vegetation biomass reported in this study could be attributed to a collection of factors: differences in scales of measurements, timing of data acquisitions, sensor properties, presence of dead biomass within the canopy, and submerged conditions. As a result of these limitations, VIs derived from spectral signatures are less effective than the lidar height metrics for predicting salt marsh vegetation biomass. However, it will be necessary to investigate this concept further using different datasets and studies across other environments.

2.5.5 Fusion of lidar and multispectral data for vegetation biomass predictions

Lidar data are capable of providing direct measurements on the vertical structure of vegetation. Further, if interpolated using appropriate data and methods, they can also be predictive of vegetation cover, particularly properties such as stem density (Lefsky *et al*. 1999; Næsset 2002; Næsset and Bjerknes 2001), percent vegetation cover, and/ or canopy openings (Nelson 1988; Weltz *et al*. 1994). However, they are incapable of providing information relating to the vegetation biophysical parameters such as the level of photosynthetic activity. In contrast, VIs derived using spectral signatures, although do not providing direct measurements on vegetation structure, are highly sensitive to the changes in vegetation condition, particularly to vegetation greenness, photosynthetic activity, and leaf moisture content (Prince *et al*. 2009; Sellers 1985; Tucker 1980), the factors that collectively control the amount of biomass available over a given area. However, their applicability is largely determined by various other factors including environment and background conditions of the vegetation and therefore can limit their use, particularly in salt marsh environments.

In this study we hypothesized that the fusion of lidar with multispectral data yields superior results for predicting salt marsh vegetation biomass as compared to each method separately. As expected, the data fusion approach improved regression models for predicting both live and dead, and thus total vegetation biomass. The fusion approach reported relatively larger improvement for the prediction of total biomass when compared to the use of lidar alone, with r^2 values increasing from 0.13 to 0.33. Thus, our results indicate the necessity of integrating multispectral signatures with the lidar

data, particularly as a surrogate for the cover type measurements in predicting vegetation biomass under short/ herbaceous vegetation with high ground cover. Similar findings have been reported in forestry. In their meta-analysis of forest biomass using lidar, Zolkos *et al*. (2013) showed that the fusion of metrics from multiple sensors produced biomass models with high accuracy. Their findings further revealed that multi-sensor fusion can produce models with accuracy levels similar to or better than those of lidar alone. Although, the improvements in regression models reported in our study are marginal, we believe these results are promising. Even though this has been researched intensely in forestry, we are not aware of any empirical study attempted using lidar or a data fusion approach to predict salt marsh vegetation biomass. While acknowledging the limitations discussed above, we believe that if the methods we present in this study are applied on detailed and high accuracy data (i.e. high point density discrete return and or/ waveform lidar data) these relationships will significantly improve. Further, such models will provide increased capability to map and characterize both spatial and temporal variations in salt marsh biomass and thus carbon, allowing us to understand the specific roles of these important terrestrial carbon sinks in the global carbon cycle. These models will also be applicable in different environments where similar vegetation characteristics exist. Given the considerable levels of accuracies (% RSE <20) reported in this study, we can infer that the estimates from these models will serve as superior to the existing estimates, which are based on generalizations over very large areas and are drawn from local scale site-specific findings. However, considering the spatial scale of this study, we believe that it is important to verify their accuracies across different sites

and using similar datasets, before implementing them at regional scales. In this study, we did not attempt to expand our study area to regional scale, mainly due to time and resource limitations.

3. THE ROLE OF ELEVATION AND RELATIVE SEA LEVEL HISTORY IN DETERMINING CARBON DISTRIBUTION IN SPARTINA ALTERNIFLORA DOMINATED SALT MARSHES

3.1 Overview

Salt marshes are among the most productive ecosystems on earth, and represent a substantial carbon sink. An understanding of the spatial patterns in the distribution of both above- and below-ground carbon in these wetland ecosystems is of critical need considering their potential in carbon sequestration projects, as well as for conservation efforts in the context of a changing climate and a rising sea. Through the use of extensive field sampling and remote sensing data (lidar and aerial images), we sought to map and explain how vegetation biomass and soil carbon are related to elevation and relative sea level change in a salt marsh in Galveston, Texas. The specific objectives of this study were to: 1) understand the relationships between elevation and the spatial patterns in the distribution of *Spartina alterniflora* vegetation characteristics and above- and below-ground carbon quantities; and 2) to investigate the possible linkages between the temporal changes in the: soil carbon deposition, relative sea level history and vegetation transitions. Our results indicated a clear zonation of terrain and vegetation height, cover and the distribution of biomass quantities within the marsh extent. Distribution of biomass quantities revealed linkages with the elevation suggesting that flood tides may be exporting material from the lower elevations to the higher elevations over time.

In general for the soil profile, the percent carbon decreased with depth, while the bulk density increased. However, both percent carbon and bulk density showed significant and abrupt change in the profile at a depth of ~10-15cm. This apparent transition in the soil characteristics coincided temporally with a transformation of the land cover, as driven by a rapid increase in relative sea level around this time at the sample locations. The amounts of soil carbon stored in recently established *Spartina alterniflora* intertidal marshes were significantly lower than those that have remained in situ for a longer period of time. These findings indicate that, even though salt marshes can respond to relative sea level rise by migrating landward, their status as a carbon sink varies as a function of both space and time. Thus, in order to predict carbon in a wetland, researchers need to know not only the elevation, the relative sea level rise rate, and the accretion rate – but also the history of land cover change and vegetation transition.

3.2 Introduction

Coastal salt marshes are among the most productive ecosystems on earth (Mitsch and Gosselink 2000) and comprise approximately 25% of the global soil carbon sink (Chmura *et al*. 2003). These salt marshes can continuously sequester carbon through plant production and burial process associated with the sea level rise. The rates of atmospheric carbon sequestration in salt marshes are likely an order of magnitude higher than that of terrestrial forests (Bridgham *et al*. 2006; McLeod *et al*. 2011; Nellemann *et al*.2009). However, uncertainties exist in the estimates of global extents of coastal salt

marshes, and their rates of carbon sequestration can vary widely both spatially and temporally.

Although some previous studies report that tidal coastal wetlands respond to sea level rise by expanding landward (Gardner *et al*. 1992; Warren and Niering 1993; Donnelly and Bertness 2001; Gardner and Porter 2001), accreting vertically (Redfield and Rubin 1962; DeLuane 1983; Callaway *et al*. 1997; Orson *et al*. 1998), and on some coasts by expanding seaward as well (Yang 1999; Shaw and Ceman 1999; Kirwan *et al*. 2010), how these changes affect their spatial distributions, carbon sequestration ability, and the carbon storage both in above- and below-ground environments still needs to be studied. Further, to understand the specific roles of each salt mash environment in the carbon cycling process, it is important to investigate the spatial and temporal variations in their patterns of above- and below-ground carbon distributions.

In general, coastal salt marshes are characterized by mild slope terrains and occur over a narrow elevation range spanning mean high water. A large number of previous studies reported elevation as an important factor that determines the spatial distribution of salt marsh vegetation communities (McKee and Patrick 1988; Pennings and Callaway 1992; Brewer *et al*. 1997; Morris *et al*. 2002; Mudd *et al*. 2004). In general, lower elevations where optimum conditions for the salt marsh plant growth available, are characterized by relatively taller and high productive vegetation communities. However, the spatial patterns in the distribution of vegetation characteristics and thus the above- and below-ground carbon can vary largely depending on different factors specific to each local environment. Thus, better understanding of the spatial patterns in the

distribution of salt marsh vegetation, and above- and below-ground carbon particularly in relevance to the elevation distribution will enable us to better understand and predict the consequences of relative sea level rise on the stability of these coastal salt marshes in terms of their spatial extents and as important carbon sinks.

Even though these wetland ecosystems are recognized to have evolved in response to sea level rise (Delaune *et al*. 1983; Pethick 1981), a rapid change in their spatial extent or composition are expected even from a small rise in the relative sea level (Warren and Niering 1993, Craft *et al*. 2009). For example, assumptions of a static landscape inspire predictions that 20-60% of the world's coastal wetlands will submerge in response to sea level rise during this century (Nicholls *et al*. 2007; Craft *et al*. 2009). Among other coastal wetlands, tidal marshes are recognized to be highly susceptible to sea level rise (Kirwan *et al*. 2010; Fagherazzi 2013), but how this change will affect ecosystem carbon storage is almost completely unknown beyond Marsh Equilibrium Model (MEM) estimates (Morris *et al*. 2002, 2012). The current rate of global sea-level rise is reported to be around 0.26 – 0.82 cm per year (IPCC 2013). While some marshes are accreting fast enough to keep up with this rise in sea level, in other places they are drowning due to local subsidence (eg, Syvitski *et al*. 2009, Yeager *et al*. 2012, Feagin *et al*. 2013).

Several studies have shown that tidal coastal wetlands respond to sea level rise by expanding landward (Gardner *et al*. 1992; Warren and Niering 1993; Donnelly and Bertness 2001; Gardner and Porter 2001) or by accreting vertically (Redfield and Rubin 1962; DeLuane 1983; Callaway *et al*. 1997; Orson *et al*. 1998). Thus, in coastal salt

marshes, over relatively long time periods, significant changes in the above- and below ground environments could be expected under the influence of relative sea level rise and at relatively higher marsh accretion rates. These changes in both physical and biotic factors will affect the marsh productivity and thus the carbon distributions. For these reasons, coastal wetland soils are studied extensively to estimate the rates of vertical accretion resulting from marsh sedimentation (Baumann *et al*. 1984; Mitsch and Gosselink 1984; Stoddart *et al*. 1989), and organic accumulation (McCaffrey and Thomson 1980; Nyman *et al*. 1993; Callaway *et al*. 1997; Anisfeld *et al*. 1999; Turner *et al*. 2004; Chmura and Hung 2004). Further, several other studies link these findings with the rates of sea-level rise (Redfield and Rubin 1962; Orson *et al*. 1998). However, the temporal variations in their spatial distribution as well as the effects of these processes on marsh build up over time and space can vary largely depending on the specific conditions that each wetland experience.

In this study, through the use of extensive field sampling and remote sensing data (lidar and aerial images), we sought to map and explain how vegetation biomass and soil carbon are related to elevation and relative sea level change using data from a *Spartina alterniflora* dominated salt marsh in Galveston, Texas. The specific objectives of this study were to: 1) understand the relationships between elevation and the spatial patterns in the distribution of *Spartina alterniflora* vegetation characteristics and above-and below-ground carbon quantities; and 2) to investigate the possible linkages between the temporal changes in the: soil carbon deposition, relative sea level history and vegetation transitions.

In this paper, we first discuss the spatial variations of vegetation characteristics and above- and belowground biomass of *Spartina alterniflora* over the study area. In doing this, we also evaluate their relationships to the variations in marsh surface elevation. In the later part, we attempt to investigate the effects of relative sea level history and resulting vegetation transition on the distribution of soil carbon in the soil profile.

3.3 Methods

3.3.1 Study area

The study area is composed of tidal salt marshes along several kilometers of shoreline (approximately 10km^2 extent) on the south side of West Galveston Bay on Galveston Island, Texas, USA. West Galveston Bay is a relatively shallow bay, with its deepest portions approximately 3m deep. It connects to the Gulf of Mexico via San Luis Pass on the southwestern end, while it connects to central Galveston Bay at the northeastern end (Figure 3-1). However, bathymetric and geographic features (e.g., the Texas City Dike and Pelican Island on the east side) prevent propagation of oceanic waves from outside West Galveston Bay. The majority (87%) of the shoreline is natural (i.e., not affected by anthropogenic activities such as dredging, dredged material disposal, filling for development, etc (Ravens *et al.* 2009). The natural shoreline of West Galveston Bay mainly consists of salt and brackish water marshes (78%). The low marshes (as influenced by daily tides) in our study area were dominated by *Spartina alterniflora*, commonly known as smooth cord grass. It is one of the most abundant salt

marsh dominant species in the intertidal zone along the coast of the northern Gulf of Mexico and the Atlantic Coast of North America. For example, *Spartina alterniflora* dominated communities are reported to contribute up to 80% of the total carbon production of Atlantic and Gulf of Mexico estuarine systems (Turner 1976).

The Galveston Island is a barrier island. The NRCS (2008) classifies these soils as gulf coast saline prairies soils. These soils are characterized by light-colored sandy soils, with very shallow soil surfaces at or only a few feet above sea level and therefore show very slow surface drainage. These soils are formed in quaternary sediments on nearly level coastal areas including coastal marshes, tidal flats, and barrier islands. Soils are mostly basic. However, our soil samples did not report the presence of any carbonates.

3.3.2 Data

3.3.2.1 Vegetation height, cover and biomass measurements

Field sampling was conducted from June 4 - 8, 2012. In locating sampling points across the study area, we employed systematic random sampling. Nineteen transects were established randomly in the *Spartina alterniflora* zone (Figure 2-1), with each extending from the water line to the landward extent of the zone (stopping before the upper reaches of the low marsh dominated by species such as *Salicornia virginica* and *Batis maritima*, salt panne species, or the un-vegetated salt panne itself). Average spacing between transects were from 50m to 100m.

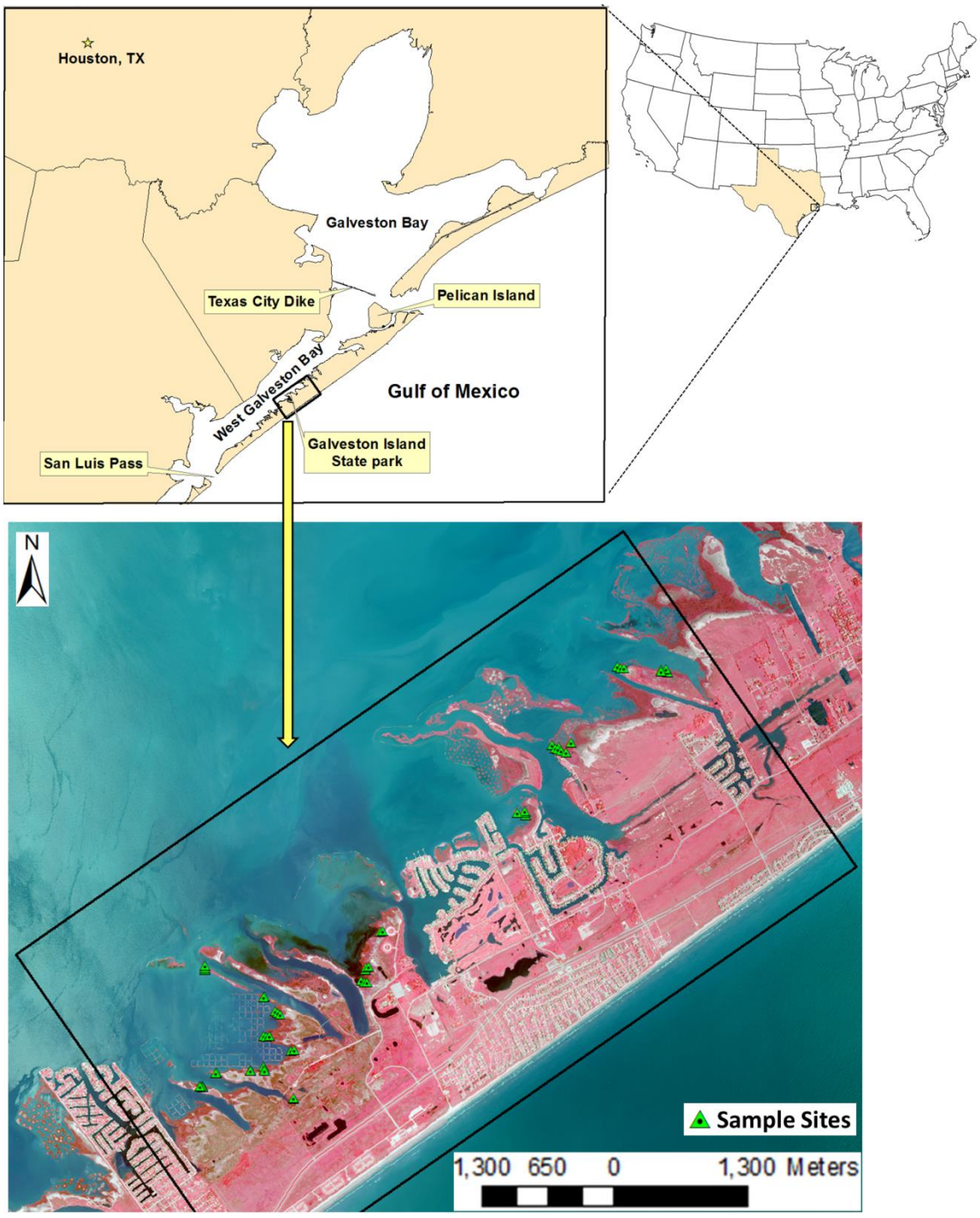

Figure 3-1. Map of the study area. Sample locations are displayed on high resolution aerial imagery acquired in June 2012. Near-infrared, red and blue bands are displayed using red, green and blue, respectively.

We assumed that the variation in vegetation height and cover conditions was determined by the gradients of elevation and tidal range. Thus, to capture the gradients of elevation, tidal range, and the observed heterogeneity in vegetation height and cover, sample plots were located systematically on these transects using 1mx1m quadrats. These quadrats were located only in mono-specific stands of *Spartina alterniflora*. The number of sample plots on each transect varied from 3 to 7 depending on the width of the *Spartina alterniflora* zone.

In the field, following standard methods (Anderson 1986) we first estimated the percentage of canopy cover within each plot visually. All the plants within the quadrats were then clipped at the ground surface. Clipped vegetation was sorted as live plants and dead vegetation/litter, placed in pre-labeled plastic bags, and transported to the lab. In the lab, plant and stem heights of individual plants were measured. Numbers of stems per quadrat were also recorded. These measurements were used to derive statistics relating to plot level field vegetation heights and density.

Clipped plants were then processed and analyzed for vegetation biomass (g dry weight per m^2) and carbon estimates, separately for live plants and dead plant material. A total of 15 samples were selected to represent the entire study area and were analyzed by combustion/gas chromatography using a Carlo Erba EA-1108 elemental analyzer (CE Elantech, Inc., Lakewood, N.J.) to obtain carbon concentrations in live and dead plant materials.

During field sampling, the central coordinates of sample plots were also established using a survey-grade, Global Navigation Satellite System (GNSS) Trimble

R2 unit; the Real Time Kinematic (RTK) with infill surveying approach was used, with all points yielding errors less than 4cm horizontal and vertical. All sampled locations were vertically referenced within NAVD 88 units. We also located a total of 42 reference points (RPs) primarily on salt pannes and other open and distinguishable areas just outside the *Spartina alterniflora* zone, and at road intersections. At each point x, y, and z coordinates were recorded. These RPs were used to verify location accuracies of the aerial images, relative to their location in the field.

3.3.2.2 Soil sampling

Soil cores were collected from the center of each quadrat after carefully clipping the above-ground material, while not disturbing the soil surface. The rectangular corer (10.16cm x 10.16cm width, 25cm length, with sharpened stainless steel bottom rim for cutting through roots) was then inserted into the marsh. Soil samples were removed from the corer using a specialized extruder. No obvious compaction of the soil samples was detected. These samples were then divided into 5 cm thick sections using a sharp knife and were placed in labeled plastic bags. We labeled and retained these sections separately to analyze for soil biomass, carbon, nitrogen, and bulk density to evaluate their differences spatially as well as across different soil depths.

To determine soil bulk densities and moisture contents, a known volume of each sample was used. Bulk densities were calculated on the basis of oven-dried weight (at 65^0C for 48 hours) and reported in grams per cubic centimeter of dry weight. Separate subsamples of approximately 50g of soil were used for the analysis of root biomass. Roots were separated using flotation method. Soil samples were immersed in high

density saturated NaCl solution (density = 1.2 g/ml), to allow the roots to float to the top of the liquid. Roots were then separated manually using a tweezers under good light for illumination.

Remaining soils were air-dried and subsamples were gently crushed and passed through 2mm sieves to remove large organic and inorganic fragments, then oven dried at 65^0C for 48 hours. These subsamples of approximately 5g were ground to a fine homogenous powder using a mortar and pestle. The mortar and pestle were cleaned and dried thoroughly between samples to avoid cross contamination. Ground soil samples were placed in a muffle furnace (460°C for 8 hours) to determine the loss of organic matter on ignition (LOI). Further, a soil moisture correction was applied on the LOI results based on moisture correction factors determined using % moisture loss of the soil samples oven dried at 105^0C. A total of 15 soil samples were then selected to analyze for percent soil carbon using combustion/gas chromatography elemental analysis. Prior to soil carbon analysis, all the soil samples were tested for the presence of soil carbonates and results did not report any carbonates in our soil samples. Relationship between LOI and this analysis revealed a strong linear relationship (%C = [LOI*0.3045]+0.3671; Least square regression with r^2=0.97; $p<0.0001$; and RMSE = 0.17%). Using this relationship, LOI results were converted to soil carbon percent. These soil samples were also analyzed for carbon and nitrogen isotope contents using combustion/gas chromatography elemental analysis.

Subsamples of vegetation (live and dead) and root samples drawn from the same quadrats were analyzed similarly using elemental analysis for their percent carbon

contents. The average percent carbon values reported for live and dead vegetation, and root biomass were used for the conversion of biomass to carbon.

3.3.2.3 Remote sensing data

High resolution (0.5m) digital aerial images for June 2012 were obtained from the National Agricultural Imagery Program (NAIP). These images consists of four (4) spectral bands in blue (428-492 nm), green (533-587 nm), red (608-662 nm), and near-infrared (833-887 nm) regions of the electromagnetic spectrum. The earliest images for the study area available from the NAIP historical data archives were for 1954. These images were available in grey scale only. When we overlaid the RPs collected during ground survey, the horizontal accuracy of the 2012 aerial images was finer than 0.5m. The historical images of 1954 were geo-referenced to the 2012 image using ground control points that were clearly visible on both images. A Root Mean Square Error (RMSE) of 0.67m was maintained in geo-referencing the two sets of images, using ArcGIS (version 10.1) software.

We also obtained Light Detection and Ranging (lidar) data that was acquired in August 2006 by the Sanborn Mapping Company, Colorado Springs, Colorado, through the use of a laser mounted on an aircraft flying at 900m height. Lidar data was used to interpolate Digital Terrain Models (DTMs) at 3m spatial scale. These DTMs were then used to understand the patterns of elevation variation over the study area, particularly within the *Spartina alterniflora* extent. Elevation accuracies of the lidar derived DTMs were also evaluated using elevation measurements of the sample points and RPs collected during the ground survey. Surface elevations of the sample locations varied

within the range from 20 to 57 cm. After evaluating the elevation variations over our study area (using 3m DTMs), we defined three elevation zones as 1) less than 30cm; 2) 30-40cm and 3) greater than 40cm. Sample locations were grouped into these respective zones, based on their ground surveyed elevation readings.

Using the 1954 and 2012 imagery, we visually evaluated transitions in the dominant vegetation type over the time period from 1954-2012. When our quadrat point locations were overlaid on to the two sets of images, we observed that the present day *Spartina alterniflora* locations were historically covered by three different land cover classes in 1954; 1) *Spartina alternlifora* dominated low marsh - LM, 2) salt pannes - SP, and 3) high marsh - HM. We then reconciled changes in the apparent aboveground vegetation cover at each point with our records of soil carbon and bulk densities, with reference to soil depth. We also evaluated current *Spartina alterniflora* plant height, maximum culm height, percent cover, plant density, and biomass as a function of land cover history at each point.

3.4 Results

3.4.1 Spatial variations of salt marsh vegetation characteristics, and above- and below-ground carbon

The mean plant and culm heights of *Spartina alterniflora* in our study area were 43.7±6cm, and 10.7±3.8cm, respectively (Table 3-1). During field measurements, we observed a gradual decrease in mean plant height along the elevation gradient, as elevation increased ($p=0.008$). The culm height difference between three zones followed

the same trend ($p<0.0001$). However, the percent vegetation cover increased with increasing elevation ($p=0.009$). Plant density, in terms of the number of stems per m^2, generally decreased with increasing elevation, though not strongly due to high variability about the mean value ($p=0.68$).

Mean aboveground biomass for our study area was 882g dry weight per m^2. Live and dead biomass components accounted for 61% and 39% of the total vegetation biomass, respectively. Percent carbon quantities (g carbon per 100g dry weight) of live and dead vegetation components were 41.3 and 34.5, respectively. Live and dead biomass quantities showed significant differences among the three elevation zones, however each followed an opposing trend along the elevation gradient; live biomass quantities decreased as elevation increased, while dead biomass increased. As a result, the total biomass showed a relatively uniform distribution with respect to elevation.

Soil carbon and nitrogen concentrations of the top 15cm soil were not strongly related to elevation ($p=0.22$ and 0.88, respectively). However, the soil C:N ratio showed significant differences across the three elevation zones ($p=0.01$), increasing with increasing elevation, similar to the trend in dead biomass accumulation.

Table 3-1. Spatial variations of vegetation characteristics and above- and belowground biomass along the elevation gradient across *Spartina alterniflora* extent.

			Elevation (cm)			
		all samples	<30	30-40	>40	Pr>ChiSquare
Plant height mean (cm)		44.7	48	44	43	0.008
Culm height mean (cm)		10.7	14	12	8	<0.0001
% Cover		86.8	82	81	93	0.009
Plant density		356	351	360	344	0.68
Above-ground C (g/m^2)	Live	219	251	222	200	0.04
	Dead	121	80	88	168	0.0004
	Total	340.6	331	310	367	0.18
Below-ground C	Root C (g/m^2)	6.6	7.9	6.5	6.0	0.97
	Soil C (g/kg soil)	29	32	26	29	0.22
	Soil N (g/kg soil)	25	26	25	25	0.88
	Soil C:N	16.2	15.3	16.0	16.8	0.01
	$\delta^{13}C_{V\text{-}PDB}$ (‰)	-18.2	-18.7	-18.1	-18.0	0.03
	$\delta^{15}N_{AIR}$ (‰)	1.7	1.42	1.78	1.85	0.18

3.4.2 Temporal changes: Soil carbon, relative sea level history and vegetation transition

Overall, the percent carbon stored in the soil profile indicated a clear depletion along the soil depth; surface soils had the highest soil carbon percentages, while they were the lowest in deeper layers. Soil bulk density showed a similar, but opposing pattern (Figures 3-2a & 3-2b). Soil carbon quantities (gC per kg soil) was more variable among deeper portions of the soil profile ($p=0.03$), whereas the soil bulk density was more variable at shallower depths ($p=0.01$). When converting via multiplication, the soil carbon storage on an aerial basis (gC per m^2) did not reveal this pattern of variation (figure 3-2c). For soil carbon storage itself, there was an apparent division between sampled layers at depths of 0-15 cm versus 15-25 cm ($p=0.001$). Considering the apparent shift in percent soil carbon below 15 cm and the shift in bulk density at this same depth, a change appears to have occurred at the corresponding time in the history of the soil's development through sediment and/ or organic matter accumulation on the marsh surface.

The dominant vegetation zones shifted their spatial locations across the salt marsh extent from 1954 to 2012. The majority of *Spartina alterniflora* dominated low marsh areas that we sampled in 2012 were of a different vegetation type in 1954 (Figure 3-3). The majority of our sample points, nearly 70% of them, were located on former salt pannes and high marshes. These observations suggest changes in relative sea level history leading to landward shift of the salt marsh extents over this 58 year period.

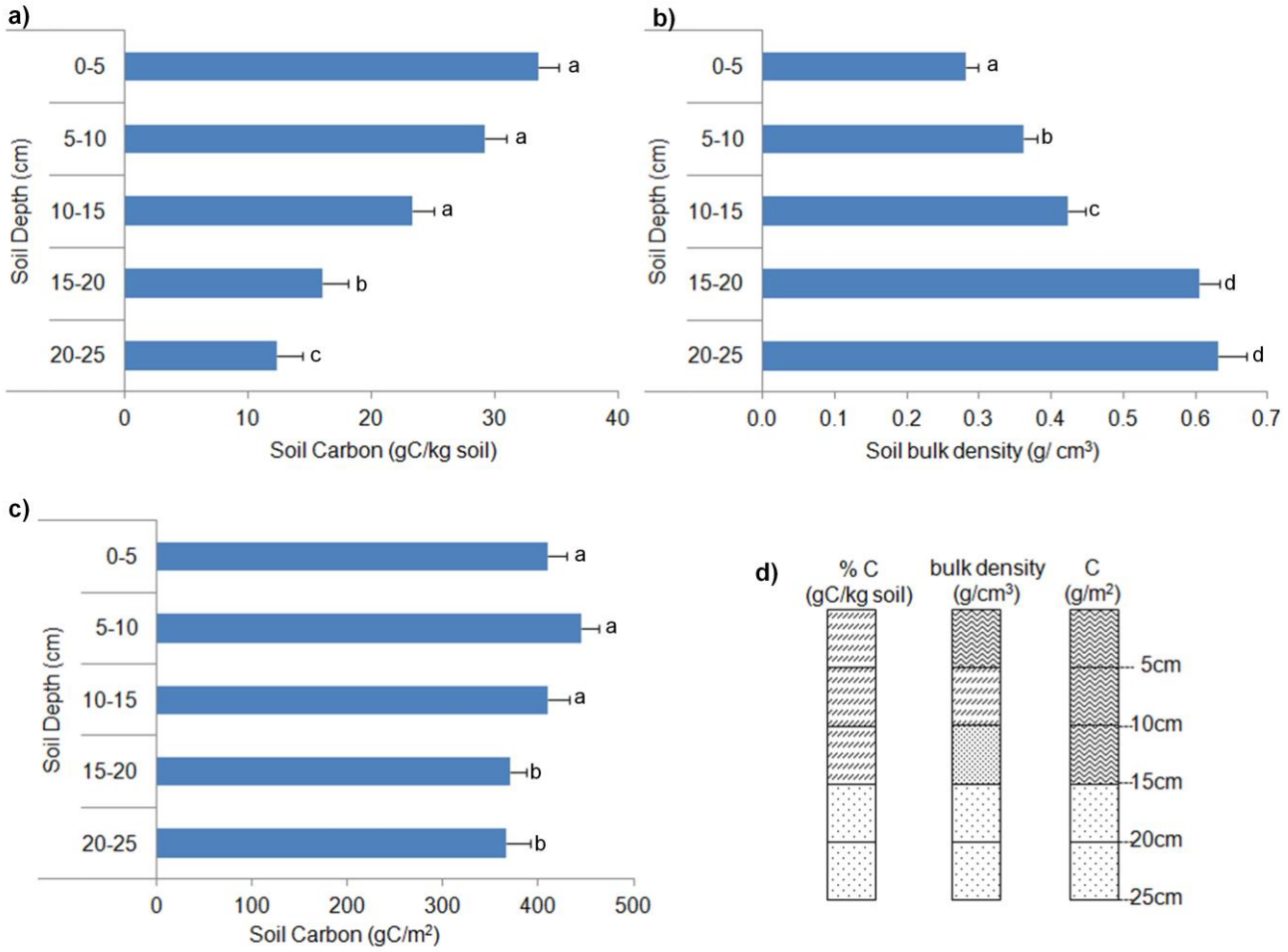

Figure 3-2. Soil carbon and bulk density variations across different depths of the soil profile(a, b, & c), and hypothetical drawing to show the variation of soil properties at different depths of the soil profile (d). Similar patterns reveal non-significant changes.

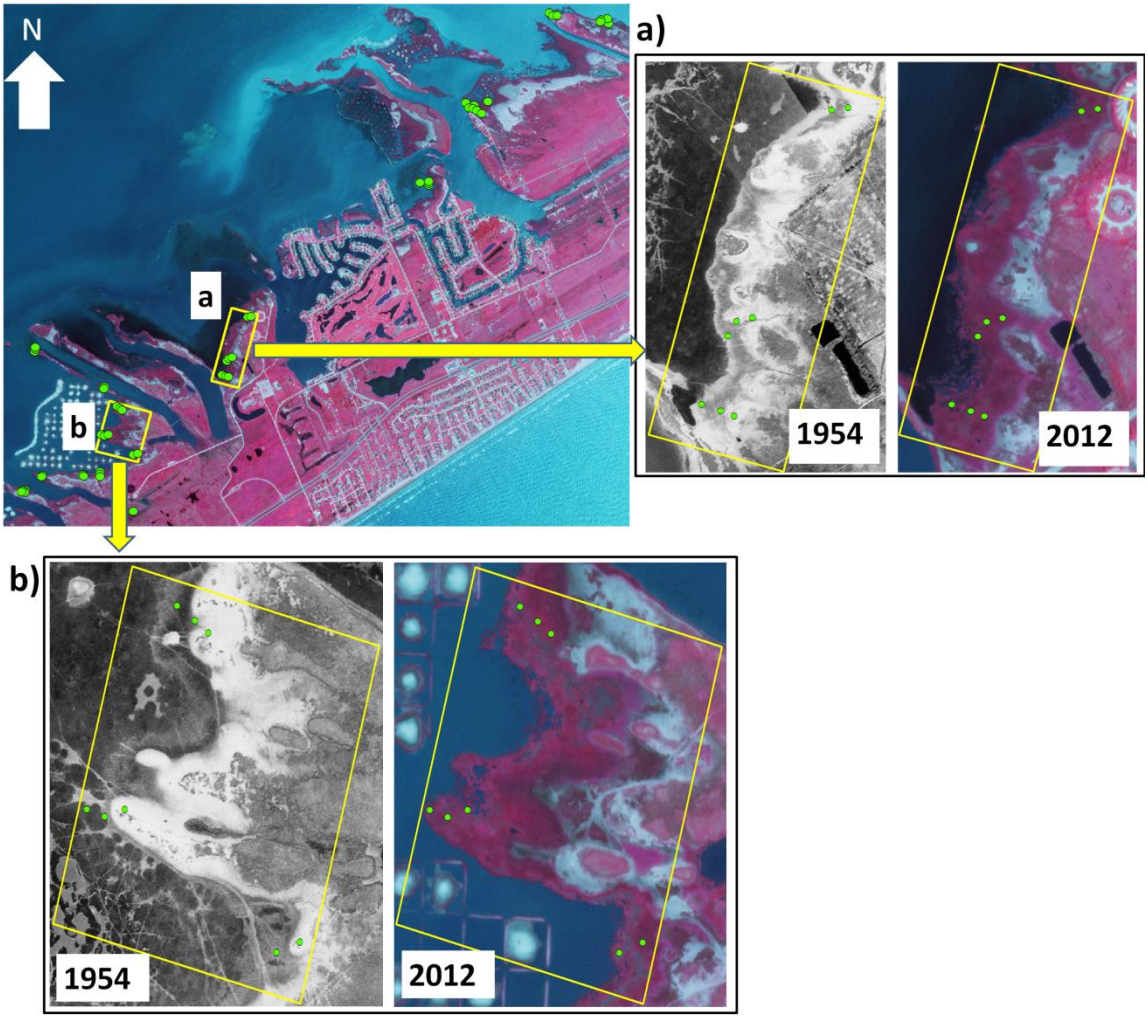

Figure 3-3. Land cover differences between two time periods. Sample points are overlaid on 2012 NAIP imagery displayed using bands NIR, red and green using red, green and blue (top left). Closer view of the two sample areas to highlight the landward shift of *Spartina alterniflora* low marsh extents and the relative sea level rise during the 58 year time period from 1954 to 2012 (a & b).

Accordingly, the trend of soil composition across depth, varied in a manner related to each of the three historical land cover types (Figure 3-4). For points that were low marshes in 1954 as well as in 2012, the 0-5cm and the 5-10cm depths were nearly identical in terms of soil carbon concentration and bulk density. Carbon concentrations decreased more slowly with depth, with a range from 40 to 20 gC/kg soil. Bulk density slightly increased with soil depth, but only up to ~0.25 g/cm^3. Further, the change in percent soil carbon was significant ($p=0.01$) only at the depth of 20cm, and the soil bulk density change was not significant at any of the depths ($p=0.05$). These bulk density values are comparable to previously reported values for coastal salt marsh soils (Callaway *et al* 1997; Feagin *et al* 2009).

Sample points from former salt pannes showed a sudden drop in soil carbon concentration and increase in bulk density at 5cm ($p=0.002$, $p=0.009$, respectively), and 15cm depths ($p<0.001$). The variation in soil carbon from the surface to the depths was much greater than the former low marshes as well, from 40 to 10 gC/kg soil. However, the soil carbon concentration at the top of the surface (0-5cm) did show similarity between former salt panne areas and former low marsh areas; points from either of these history types showed a higher soil carbon concentration as compared to the former high marsh areas at the surface only (an approximately 1% difference in soil carbon concentrations), suggesting that their current elevation position is the determinant in that top layer (as compared to the former high marsh locations that were in 2012 among the highest elevation points). Soil parameters in the deeper soil layers (below 5cm soil layer) did not show significant differences between the soil cores of former salt panne

and former high marsh areas. As compared with the former low marsh areas, the deepest layer of the salt panne was much poorer in percent carbon (about half at the 20-25 cm layer), and moderately higher in bulk densities. Interestingly, the former high marshes had their minimum percent carbon value and maximum bulk density at the 15-20 cm layer, rather than the 20-25 cm layer, suggesting a possible transition from a former high marsh into a salt panne, and then finally into a low marsh at the upper layers.

Comparatively, sample points historically covered by low marshes reported significantly higher percentage of soil carbon as compared to the sample points that were converted to low marshes after 1954 ($p=0.003$), for the top 15cm soil. Considering the entire soil profile, the soil carbon quantities for law marshes, salt pannes, and high marshes were 34.5, 27.4, and 23.0 gC per kg soil, respectively. Further, former low marsh areas had the highest absolute quantities of soil carbon (gC per m^2) storage at all depths.

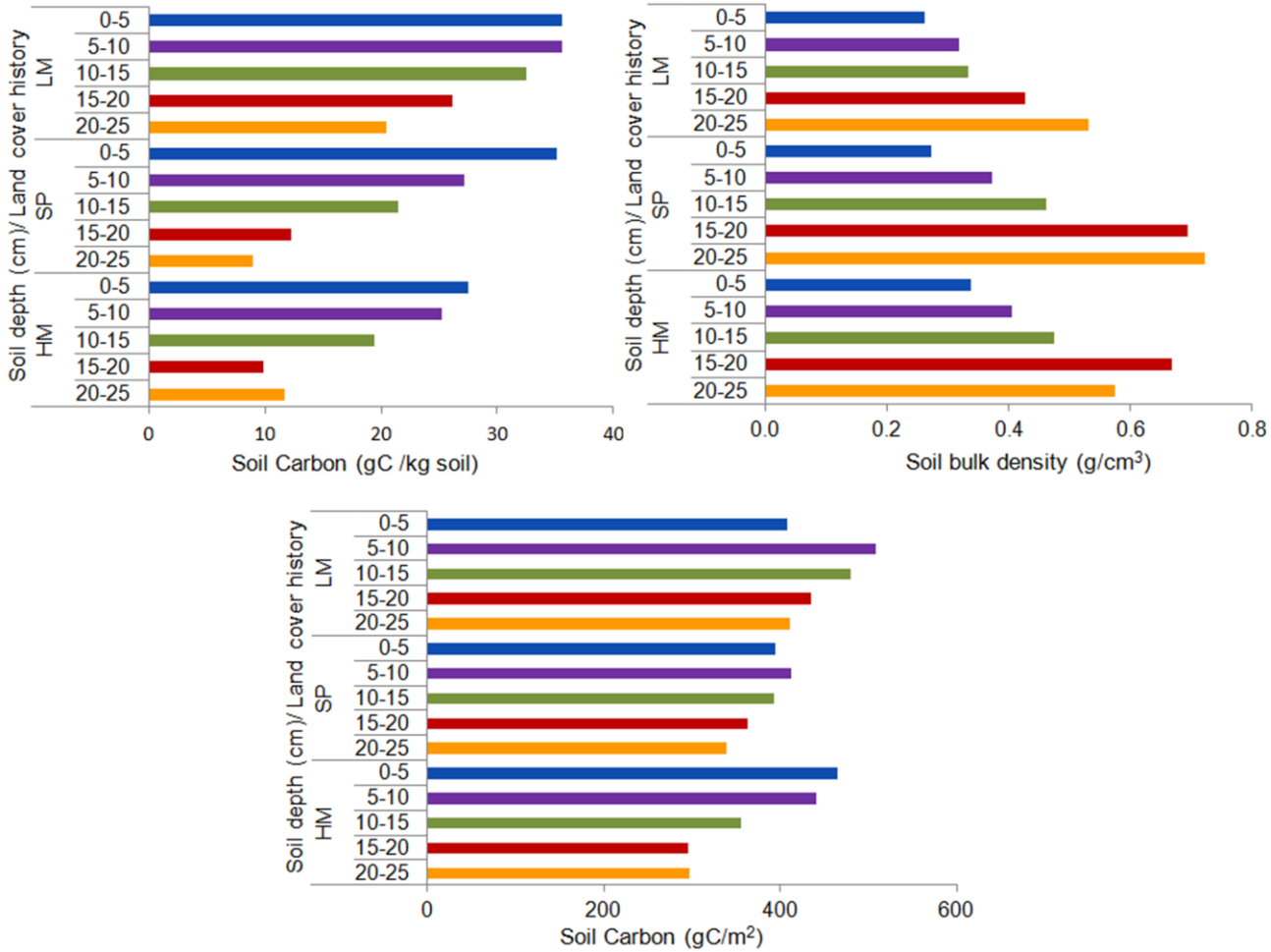

Figure 3-4. Figure 3-4. Soil carbon and bulk density changes along the soil profile separately for the three sample groups defined based on the historical land cover identified for each of the sample locations; 1) HM - high marsh, 2) SP - salt pans, and 3) LM - low marshes.

3.5 Discussion

3.5.1 Spatial variations of salt marsh vegetation characteristics, and above-and below-ground carbon

Spartina alterniflora vegetation height varies along the elevation gradient, as shown empirically in the present study and in previous studies (Hardisky *et. al.* 1984, Pennings and Callaway 1992; Castillo *et. al*. 2008). Though our site did not exhibit the typical short versus tall *Spartina alterniflora* phenotypic expression that is often seen in other studies, we did witness taller plants and culms in lower elevations on the seaward edges of the marsh. Elevation plays a major role in determining the direct influence of tidal height and thereby the distribution of soil nutrients, suspended sediment supply, and anoxic conditions within the marsh environment (DeLaune *et al*. 1983a & b; Silvestri *et al*. 2005). Studies have shown evidence for direct linkages between elevation and pore water salinity (Moffett *et. al*. 2010), which is recognized to be an important controlling factor on vegetation distribution. Present-day elevation likely is the predominant factor driving aboveground and belowground plant characteristics and biomass.

The above-ground biomass quantities of *Spartina alterniflora* reported to be in the range from 100 – 3700 g dry weight per m^2 (Castillo *et al*. 2010). The values reported in our study area varied within a narrow range from 304 to 1452 g dry weight per m^2. However, these values are comparable with the biomass measurements reported for this area. For example, Webb and Newling (1985) reported *Spartina alterniflora* biomass quantities ranging from 22 to 936 g dry weight per m^2 for the salt marshes in

Galveston Bay complex which include our study area. Also, in a different study, Hardisky *et al*. (1984) reported similar values for *Spartinal alterniflora* salt marshes over the North Gulf coast of US.

The total biomass carbon (live + dead) was distributed relatively evenly across elevation. However, this evenness does not necessarily mean that the process that occurs at low and high elevations is the same. In general, the lower elevations in our study were characterized by more robust growth with erect, few stems emerging from clumps, while the upper elevations had a short dense layer of overlapping vegetation canopies consisting largely of dead leaves and stems from the previous season. We observed a greater amount of dead biomass accumulation at upper elevations. Thus, while the total biomass carbon stock is relatively evenly-distributed across the elevation gradient and not statistically differing with respect to elevation, newly emerging plants are contributing to live biomass at the lower elevations and then exporting this material to the higher elevations.

Corroborating this hypothesized process, the soil C:N ratio increased with increasing elevation. In general, dead plant matter are characterized by relatively higher C:N ratios compared to live matter. Early studies reported lower decomposition rates in the organic matter characterized by high C:N ratios, which are resistant to decay. This lower decomposition rates in turn, could explain the lower percentage of soil carbon at the highest elevations, regardless of the increased accumulation of organic matter on the marsh surfaces. The material from lower elevations is exported to and accumulated at higher elevations, some of that carbon is then integrated into the soil, and the remainder

is exported to even higher elevations on subsequent tides. Thus, there is a spatial-averaging of carbon across the landscape, and with respect to elevation, that is driven by the tide continually moving dead biomass to higher elevations.

3.5.2 Temporal changes: soil carbon deposition, relative sea level history and vegetation transition

The primary mode of vegetation transition over the 58 year period (1954-2012) was a landward shift of the salt marsh extent. Much work has been devoted to understanding how this zonal migration process is related to relative sea level rise. As the sea level rises at a given point location, the marsh responds through a coupled accretion process (Morris *et al*. 2002), and if there is an accretionary deficit, then the low marsh may be lost at a specific point due to inundation(Cahoon *et al*. 2006; Nyman et. al. 2006; Connor et. al. 2001). Across the landscape, the zones of the marsh appear to migrate landward to higher elevations (Feagin *et al*. 2008). When barriers prevent this migration, the marsh is lost, and findings from around the US have indicated a significant loss of coastal salt marshes due to these processes over the last century (USFWS 2011, 2013).

Marsh loss and zonal migration at our study site has been extensive over the last century, and is due to an insufficient sediment supply and accretion rate, as compared to the relative sea level rise. Immediate to our study area in the Galveston Island State Park *Spartina alterniflora* low marshes, Feagin *et al*. (2005) and Feagin *et al*. (2010) reported relative sea level rise rates of 0.65 cm per year and Ravens *et. al.* (2009) reported sediment accumulation rates ranging from 0.14 to 0.36 cm per year. More generally in

this hydrologic basin, White *et. al*. (2002) reported an average sedimentation rate of 0.5cm per year, while Yeager *et. al*. (2007), for a different wetland in the same region reported a sedimentation rate of 0.16cm per year. Processes driving the accretionary deficit in this region include lowered sediment supply due to the construction of the Texas City Dike, the damming of inflowing rivers, subsidence driven by the fault activation as due to water and hydrocarbon extraction, regional autocompaction, and eustatic sea level rise (White and Morton 1997). As a result, White *et. al*. (1995) reports a loss of about 12% salt marshes on the Galveston coast between 1950 and 1989, while Glass and Hollingsworth (1999) indicated a loss of 405ha in Galveston Island State Park (encompassed by our study area) alone between 1930 and 1994.

There were two distinct and significantly different layers found in the general results of our core profiles: (1) a surface layer to ~15cm depth characterized by higher soil carbon concentrations and lower soil bulk densities, and (2) a layer below ~15cm with lower soil carbon concentrations and higher soil bulk densities. Interestingly, multiplying an average accretion rate of ~0.25 cm per year at this site (from Ravens. 2006), by ~58 years (1954-2012), yields ~15 cm of soil depth – a number that coincides with this transition depth. This transition was particularly evident in the bulk density and soil carbon (g C per m^2) profiles of the former salt panne and high marsh cores at the 15-20 depth. However, soil cores of former low marshes did not show this transition in soil carbon until the depth of 20-25cm. Further, in this group, up to 25cm depth mean soil bulk density of low marshes did not reveal significant differences at any depth. Thus, in our work, there appear to be clear linkages between the relative sea level rise

rate, accretion rate, and vegetation transition across the landscape. Accordingly, the shifting vegetation types altered the bulk density of the soil and the quantity of carbon that was deposited.

3.5.3 Hypothesized rules for spatial and temporal carbon deposition in *Spartina alterniflora* marshes

Summarizing for *Spartina alterniflora* marshes, we hypothesize that carbon distribution should follow these general rules: (1) live biomass carbon decreases with elevation, (2) dead biomass carbon increases with elevation, (3) total biomass carbon is generally even across elevation, due to the spatial averaging of tidal export/import of dead biomass, (4) soil carbon is affected by this spatial averaging process and high C:N ratios in the above ground dry plant material limited the incorporation of this carbon into the soil due to the slow decay rates, (5) soil carbon decreases with depth, due generally to oxidation and the concentration of organic matter and plant roots in the surface of the soil profile, (6) soil carbon at depth is linked to land cover history: greatest in low marshes, then high marshes, with salt pannes the lowest, (7) soil carbon decreases as the accretion deficit increases, due not only to the lack of deposition but also to the likelihood that the location was not a *Spartina alterniflora* low marsh in the past.

4. CONCLUSIONS

This study evaluated the capabilities of the integration of remote sensing data (lidar and multispectral) and techniques with field measurements for the quantification of carbon pools in salt marsh ecosystems using the data from a *Spartina alterniflora* dominated coastal salt marsh in Galveston, Texas, USA.

The first part of this study (Chapter 2), evaluated the increased capabilities of a data fusion approach using lidar and multispectral remote sensing data to provide accurate estimates on salt marsh terrain, vegetation height, cover, and above-ground biomass and carbon quantities. Evaluation of the accuracies of salt marsh DTMs derived using different approaches and at varying grid sizes indicated that the local minima in a grid spacing of 5mx5m, provided the best accuracy in terrain elevation estimates with an RMSE of less than 10cm. Lidar-derived maximum vegetation heights (Lmax) provided the best agreement with field height measurements, but explained only 41% of the variance in vegetation height measurements (RMSE = 5.85cm). Regardless of the metrics used, lidar-measured heights underestimated the field vegetation height, which is consistent with the findings of previous studies in short or herbaceous vegetation. The fusion of lidar with multispectral data improved model predictions of live, dead, and total biomass quantities. The improvement provided by the fusion over the use of lidar or multispectral data alone was marginal; the combination explained 47% of the variance, whereas the best models using lidar and multispectral data separately explained 37% and 28% of variances in live biomass measurements, respectively. However, the

best biomass prediction models reported considerably low RMSEs and % root square errors (% RSEs). For example, % RSE for the biomass prediction model using lidar-derived maximum vegetation height (Lmax) was closer to 20%, which is the recommended error threshold for remote sensing based forest biomass prediction models that can be repeatedly applicable for estimating forest carbon stock change. Thus, our findings demonstrate that lidar as compared to spectral data can provide better estimates of above-ground biomass and carbon, even in the herbaceous and low-relief context of a salt marsh.

The second part (Chapter 3) of this study focused on the spatial patterns in the distribution of *Spartina alterniflora* vegetation characteristics and above-and below-ground carbon quantities. Further, the linkages between the temporal changes in the: soil carbon deposition, relative sea level history and vegetation transitions were evaluated. Our results indicate a clear zonation of terrain, vegetation characteristics and the distribution of biomass quantities within the marsh extent. Distribution of biomass quantities revealed linkages with the elevation. Variations in soil properties (i.e. carbon and bulk density) in the soil profile were linked to the temporal changes in soil carbon accumulations on the marsh surface, relative sea level history and resulting vegetation transitions as corroborated by historical aerial images. In general, the amounts of soil carbon stored in recently established *Spartina alterniflora* intertidal marshes were significantly lower than those that have remained in situ for a longer period of time. Our findings indicate that, even though salt marshes can respond to relative sea level rise by migrating landward, their status as a carbon sink varies as a function of both space and

time. Thus, in order to predict carbon in a wetland, researchers need to know not only the elevation, the relative sea level rise rate, and the accretion rate – but also the history of land cover change and vegetation transition.

REFERENCES

Adams, J., & Chandler, J. (2002). Evaluation of lidar and medium scale photogrammetry for detecting soft-cliff coastal change. The Photogrammetric Record, 17, 405-418

Akaike, H. (1981). Likelihood of a model and information criteria. Journal of Econometrics, 16, 3-14

Anderson, E.W. (1986). A guide for estimating cover. Rangelands, 8, 236-238

Anisfeld, S., Tobin, M., & Benoit, G. (1999). Sedimentation rates in flow-restricted and restored salt marshes in Long Island Sound. Estuaries, 22, 231-244

Asselman, N.E.M. (2002). Laser altimetry and hydraulic roughness of vegetation, further studies using ground truth. Delft Hydraulics, Q3139: WL, Delft, Netherlands.

Atjay, G.L., Ketner, P., & Duvigneaud, P. (1979). Terrestrial primary production and phytomass. The Global Carbon Cycle, 13, 129- 182.

Baltsavias, E.P. (1999). Airborne laser scanning: existing systems and firms and other resources. ISPRS Journal of Photogrammetry and Remote Sensing, 54, 164-198

Baumann, R.H., Day, J.W., & Miller, C.A. (1984). Mississippi deltaic wetland survival: sedimentation versus coastal submergence. Science, 224, 1093-1095

Belluco, E., Camuffo, M., Ferrari, S., Modenese, L., Silvestri, S., Marani, A., & Marani, M. (2006). Mapping salt-marsh vegetation by multispectral and hyperspectral remote sensing. Remote Sensing of Environment, 105, 54-67

Belsley, D.A., Kuh, E. & Welsch, R. E. (1980). Regression diagnostics: identifying influential data and sources of collinearity. New York: Wiley

Boudreau, J., Nelson, R.F., Margolis, H.A., Beaudoin, A., Guindon, L., & Kimes, D.S. (2008). Regional aboveground forest biomass using airborne and spaceborne lidar in Québec. Remote Sensing of Environment, 112, 3876-3890

Bowen, Z.H., & Waltermire, R.G. (2002). Evaluation of light detection and ranging (lidar) for measuring river corridor topography. Journal of the American Water Resources Association, 38, 33-41

Brewer, J.S., Levine, J.M., & Bertness, M.D. (1997). Effects of biomass removal and elevation on species richness in a New England salt marsh. Oikos, 80, 333-341

Bridgham, S., Megonigal, J., Keller, J., Bliss, N., & Trettin, C. (2006). The carbon balance of North American wetlands. Wetlands, 26, 889-916

Cahoon, D., Hensel, P., Spencer, T., Reed, D., McKee, K., & Saintilan, N. (2006). Coastal wetland vulnerability to relative sea-level rise: wetland elevation trends and process controls. In J.A. Verhoeven, B. Beltman, R. Bobbink & D. Whigham (Eds.), Wetlands and Natural Resource Management (pp. 271-292): Springer Berlin Heidelberg

Cahoon, D.R., & Reed, D.J. (1995). Relationships among marsh surface topography, hydroperiod, and soil accretion in a deteriorating Louisiana salt marsh. Journal of Coastal Research, 11, 357-369

Callaway, J.C., DeLaune, R.D., & Jr, W.H.P. (1997). Sediment accretion rates from four coastal wetlands along the Gulf of Mexico. Journal of Coastal Research, 13, 181-191

Castillo, J.M., Leira-Doce, P., Rubio-Casal, A.E., & Figueroa, E. (2008). Spatial and temporal variations in aboveground and belowground biomass of *Spartina maritima* (small cordgrass) in created and natural marshes. Estuarine, Coastal and Shelf Science, 78, 819-826

Castillo, J.M., Rubio-Casal, A.E., & Figueroa, E. (2010). Cordgrass biomass in coastal marshes. SCIYO. COM, 1

Chapin, F., Woodwell, G., Randerson, J., Rastetter, E., Lovett, G., Baldocchi, D., Clark, D., Harmon, M., Schimel, D., Valentini, R., Wirth, C., Aber, J., Cole, J., Goulden, M., Harden, J., Heimann, M., Howarth, R., Matson, P., McGuire, A., Melillo, J., Mooney, H., Neff, J., Houghton, R., Pace, M., Ryan, M., Running, S., Sala, O., Schlesinger, W., & Schulze, E.D. (2006). Reconciling carbon-cycle concepts, terminology, and methods. Ecosystems, 9, 1041-1050

Chassereau, J.E., Bell, J.M., & Torres, R. (2011). A comparison of GPS and lidar salt marsh DEMs. Earth Surface Processes and Landforms, 36, 1770-1775

Chmura, G.L., Anisfeld, S.C., Cahoon, D.R., & Lynch, J.C. (2003). Global carbon sequestration in tidal, saline wetland soils. Global Biogeochemical. Cycles, 17, 1111

Chmura, G.L., & Hung, G.A. (2004). Controls on salt marsh accretion: A test in salt marshes of eastern Canada. Estuaries, 27, 70-81

Choi, Y., Wang, Y., Hsieh, Y.-P., & Robinson, L. (2001). Vegetation succession and carbon sequestration in a coastal wetland in northwest Florida: Evidence from carbon isotopes. Global Biogeochemical Cycles, 15, 311-319

Chust, G., Galparsoro, I., Borja, Á., Franco, J., & Uriarte, A. (2008). Coastal and estuarine habitat mapping, using lidar height and intensity and multispectral imagery. Estuarine, Coastal and Shelf Science, 78, 633-643

Cobby, D.M., Mason, D.C., & Davenport, I.J. (2001). Image processing of airborne scanning laser altimetry data for improved river flood modelling. ISPRS Journal of Photogrammetry and Remote Sensing, 56, 121-138

Collin, A., Long, B., & Archambault, P. (2010). Salt-marsh characterization, zonation assessment and mapping through a dual-wavelength lidar. Remote Sensing of Environment, 114, 520-530

Craft, C., Clough, J., Ehman, J., Joye, S., Park, R., Pennings, S., Guo, H., & Machmuller, M. (2009). Forecasting the effects of accelerated sea-level rise on tidal marsh ecosystem services. Frontiers in Ecology and the Environment, 7, 73-78

Davenport, I.J., Bradbury, R.B., Anderson, G.Q.A., Hayman, G.R.F., Krebs, J.R., Mason, D.C., Wilson, J.D., & Veck, N.J. (2000). Improving bird population models using airborne remote sensing. International Journal of Remote Sensing, 21, 2705-2717

Davidson, N.C., & Finlayson, C.M. (2007). Earth Observation for wetland inventory, assessment and monitoring. Aquatic Conservation: Marine and Freshwater Ecosystems, 17, 219-228

DeLaune, R.D., Pezeshki, S.R., & Jr, W.H.P. (1987). Response of coastal plants to increase in submergence and salinity. Journal of Coastal Research, 3, 535-546

DeLaune, R.D., Smith, C.J., & Patrick, W.H. (1983b). Relationship of marsh elevation, redox potential, and sulfide to *Spartina alterniflora* productivity. Soil Science. Soceity of America Journal, 47, 930–935

Dixon, R.K., & Krankina, O. N. (1995). Can the terrestrial biosphere be managed to conserve and sequester carbon. In M.A. Beran (Ed.), Carbon sequestration in the biosphere: processes and products, NATO ASI Ser., Ser. I, Global Environ. Change (pp. 153-179). New York: Springer-Verlag

Donato, D.C., Kauffman, J.B., Murdiyarso, D., Kurnianto, S., Stidham, M., & Kanninen, M. (2011). Mangroves among the most carbon-rich forests in the tropics. Nature Geoscience, 4, 293-297

Drake, J.B., Dubayah, R.O., Clark, D.B., Knox, R.G., Blair, J.B., Hofton, M.A., Chazdon, R.L., Weishampel, J.F., & Prince, S. (2002). Estimation of tropical forest structural characteristics using large-footprint lidar. Remote Sensing of Environment, 79, 305-319

Duarte, C.M., Middelburg, J.J., & Caracao, N. (2005). Major role of marine vegetation on the oceanic carbon cycle. Biogeosciences, 2, 1-8

Evans, J., Hudak, A., Faux, R., & Smith, A.M. (2009). Discrete return lidar in natural resources: Recommendations for project planning, data processing, and deliverables. Remote Sensing, 1, 776-794

Feagin, R. (2013). Foredune restoration before and after hurricanes: inevitable destruction, certain reconstruction. In M.L. Martínez, J.B. Gallego-Fernández &

P.A. Hesp (Eds.), Restoration of Coastal Dunes (pp. 93-103): Springer Berlin Heidelberg

Feagin, R.A., Martinez, M.L., Mendoza-Gonzalez, G., & Costanza, R. (2010). Salt marsh zonal migration and ecosystem service change in response to Global sea level rise: A case study from an urban region. Ecology and Society, 15, 14

Feagin, R.A., Lozada-Bernard, S.M., Ravens, T.M., Möller, I., Yeager, K.M., & Baird, A.H. (2009). Does vegetation prevent wave erosion of salt marsh edges? Proceedings of the National Academy of Sciences, 106, 10109-10113

Feagin, R.A., Sherman, D.J., & Grant, W.E. (2005). Coastal erosion, global sea-level rise, and the loss of sand dune plant habitats. Frontiers in Ecology and the Environment, 3, 359-364

Gardner, L.R., & Porter, D.E. (2001). Stratigraphy and geologic history of a southeastern salt marsh basin, North Inlet, South Carolina, USA. Wetlands Ecology and Management, 9, 371-385

Gardner, L.R., Smith, B.R., & Michener, W.K. (1992). Soil evolution along a forest-salt marsh transect under a regime of slowly rising sea level, southeastern United States. Geoderma, 55, 141-157

Gaveau, D.L.A., & Hill, R.A. (2003). Quantifying canopy height underestimation by laser pulse penetration in small-footprint airborne laser scanning data. Canadian Journal of Remote Sensing, 29, 650-657

Glass, P., & Hollingsworth, T. (1999). Wetlands restoration at Galveston Island State Park a multi-agency project. In, Galveston Bay Estuary Program State of the Bay Symposium IV (pp. 201-204). Galveston, Texas

Groenendijk, A.M., & Vink-Lievaart, M.A. (1987). Primary production and biomass on a Dutch salt marsh: emphasis on the below-ground component. Vegetation, 70, 21-27

Harding, D.J., Lefsky, M.A., Parker, G.G., & Blair, J.B. (2001). Laser altimeter canopy height profiles: methods and validation for closed-canopy, broadleaf forests. Remote Sensing of Environment, 76, 283-297

Hardisky, M.A., Daiber, F.C., Roman, C.T., & Klemas, V. (1984). Remote sensing of biomass and annual net aerial primary productivity of a salt marsh. Remote Sensing of Environment, 16, 91-106

Hardisky, M.A., Gross, M.F., & Klemas, V. (1986). Remote sensing of coastal wetlands. BioScience, 36, 453-460

Hodgson, M.E., & Bresnahan, P. (2004). Accuracy of airborne lidar-derived elevation: empirical assessment and error budget. Photogrammetric Engineering and Remote Sensing, 70, 331-340

Hodgson, M.E., Jensen, J.R., Schmidt, L., Schill, S., & Davis, B. (2003). An evaluation of lidar- and IFSAR-derived digital elevation models in leaf-on conditions with USGS Level 1 and Level 2 DEMs. Remote Sensing of Environment, 84, 295-308

Holzer, T.L., & Galloway, D.L. (2005). Impacts of land subsidence caused by withdrawal of underground fluids in the United States. In J. Ehlen, W.C.

Haneberg & R.A. Larson (Eds.), Humans as geologic agents (pp. 87-99). Boulder, Colorado: Geological Society of America Reviews in Engineering Geology

Hopkinson, C., Chasmer, L.E., Sass, G., Creed, I.F., Sitar, M., Kalbfleisch, W., & Treitz, P. (2005). Vegetation class dependent errors in lidar ground elevation and canopy height estimates in a boreal wetland environment. Canadian Journal of Remote Sensing, 31, 191-206

Hopkinson, C., Lim, K., Chasmer, L.E., Treitz, P., Creed, I.F., & Gynan, C. (2004). Wetland grass to plantation forest–estimating vegetation height from the standard deviation of lidar frequency distributions. International Archives of Photogrammetry, Remote Sensing and Spatial Information Sciences, 36, 8

Howarth, R.W. (1993). Microbial processes in salt-marsh sediments. In T.E. Ford (Ed.), Aquatic microbiology: An ecological approach (pp. 239-259): Blackwell Scientific

Islam, M.A., Thenkabail, P.S., Kulawardhana, R.W., Alankara, R., Gunasinghe, S., Edussriya, C., & Gunawardana, A. (2008). Semi-automated methods for mapping wetlands using Landsat ETM+ and SRTM data. International Journal of Remote Sensing, 29, 7077-7106

Jensen, J.R., Coombs, C., Porter, D., Jones, B., Schill, S., & White, D. (1998). Extraction of smooth cordgrass (*Spartina alterniflora*) biomass and leaf area index parameters from high resolution imagery. Geocarto International, 13, 25-34

Kauffman, J.B., Heider, C., Cole, T., Dwire, K., & Donato, D. (2011). Ecosystem carbon stocks of micronesian mangrove forests. Wetlands, 31, 343-352

Komiyama, A., Ong, J.E., & Poungparn, S. (2008). Allometry, biomass, and productivity of mangrove forests: A review. Aquatic Botany, 89, 128-137

Kulawardhana, R.W., P. S. Thenkabail, J. Vithanage, C. Biradar, Md. A. Islam, S. Gunasinghe, R. Alankara (2007). Evaluation of the wetland mapping methods using landsat ETM+ and SRTM data. Journal of Spatial Hydrology, 7, 62-96

Laffoley, D., & Grimsditch, G.D. (2009). The management of natural coastal carbon sinks: Iucn

Lana, P.d.C., Guiss, C., & Disaró, S.T. (1991). Seasonal variation of biomass and production dynamics for above- and belowground components of a *Spartina alterniflora* marsh in the euhaline sector of Paranaguá Bay (SE Brazil). Estuarine, Coastal and Shelf Science, 32, 231-241

Lefsky, M.A., Cohen, W.B., Acker, S.A., Parker, G.G., Spies, T.A., & Harding, D. (1999). Lidar remote sensing of the canopy structure and biophysical properties of douglas-fir western hemlock forests. Remote Sensing of Environment, 70, 339-361

Lefsky, M.A., Cohen, W.B., Harding, D.J., Parker, G.G., Acker, S.A., & Gower, S.T. (2002). Lidar remote sensing of above-ground biomass in three biomes. Global Ecology and Biogeography, 11, 393-399

Lefsky, M.A., Harding, D.J., Keller, M., Cohen, W.B., Carabajal, C.C., Del Bom Espirito-Santo, F., Hunter, M.O., & de Oliveira, R. (2005). Estimates of forest

canopy height and aboveground biomass using ICESat. Geophysical Research Letters, 32

Leibowitz, N.C., & Brown, M.T. (1990). Indicator strategies for wetlands. In T.H.a.D.E. Carpenter (Ed.), EMAP ecological indicators. Washington, D.C., USA: Environmental Protection Agency

Lim, K., Treitz, P., Baldwin, K., Morrison, I., & Green, J. (2003). Lidar remote sensing of biophysical properties of tolerant northern hardwood forests. Canadian Journal of Remote Sensing, 29, 658-678

MacMillan, R.A., Martin, T.C., Earle, T.J., & McNabb, D.H. (2003). Automated analysis and classification of landforms using high-resolution digital elevation data: applications and issues. Canadian Journal of Remote Sensing, 29, 592-606

Magnussen, S., & Boudewyn, P. (1998). Derivations of stand heights from airborne laser scanner data with canopy-based quantile estimators. Canadian Journal of Forest Research, 28, 1016-1031

Magnussen, S., Eggermont, P., & LaRiccia, V.N. (1999). Recovering tree heights from airborne laser scanner data. Forest Science, 45, 407-422

McCaffrey, R.J., & Thomson, J. (1980). A record of the accumulation of sediment and trace metals in a Connecticut salt marsh. In B. Saltzman (Ed.), Advances in Geophysics, Estuarine Physics and Chemistry: Studies in Long Island Sound (pp. 165-236). New York: Academic Press

McKee, K., & Patrick, W.H. (1988). The relationship of smooth cordgrass (*Spartina alterniflora*) to tidal datums: A review. Estuaries, 11, 143-151

McLeod, E., Chmura, G.L., Bouillon, S., Salm, R., Björk, M., Duarte, C.M., Lovelock, C.E., Schlesinger, W.H., & Silliman, B.R. (2011). A blueprint for blue carbon: toward an improved understanding of the role of vegetated coastal habitats in sequestering CO_2. Frontiers in Ecology and the Environment, 9, 552-560

Means, J.E., Acker, S.A., Harding, D.J., Blair, J.B., Lefsky, M.A., Cohen, W.B., Harmon, M.E., & McKee, W.A. (1999). Use of large-footprint scanning airborne lidar to estimate forest stand characteristics in the western cascades of Oregon. Remote Sensing of Environment, 67, 298-308

Mendelssohn, I.A., McKee, K.L., & Patrick, W.H. (1981). Oxygen deficiency in *Spartina alterniflora* roots: Metabolic adaptation to anoxia. Science, 214, 439-441

Mendelssohn, I.A., & Morris, J.T. (2000). Ecophysiological controls on the growth of *Spartina alterniflora*. In N.P.W.a.D.A. Kreeger. (Ed.), Concepts and controversies in tidal marsh ecology (pp. 59-80). Dordrecht, The Netherlands: Kluwer

Mitsch, W.J., & Gosselink, J.G. (1984). Wetlands. Van Nostrand, NY

Mitsch, W.J., & Gosselink, J.G. (2000). The value of wetlands: importance of scale and landscape setting. Ecological Economics, 35, 25-33

Moffett, K.B., Robinson, D.A., & Gorelick, S.M. (2010). Relationship of salt marsh vegetation zonation to spatial patterns in soil moisture, salinity, and topography. Ecosystems, 13, 1287-1302

Montane, J.M., & Torres, R. (2006). Accuracy assessment of lidar salt marsh topographic data using RTK GPS. Photogrammetric Engineering and Remote Sensing, 72, 961-967

Morris, J.T., Sundareshwar, P.V., Nietch, C.T., Kjerfve, B., & Cahoon, D.R. (2002). Responses of coastal wetlands to rising sea level. Ecology, 83, 2869-2877

Mudd, S.M., Fagherazzi, S., Morris, J.T., & Furbish, D.J. (2004). Flow, sedimentation, and biomass production on a vegetated salt marsh in South Carolina: Toward a predictive model of marsh morphologic and ecologic evolution. The Ecogeomorphology of Tidal Marshes (pp. 165-188). Washington, DC: AGU

Næsset, E. (1997). Estimating timber volume of forest stands using airborne laser scanner data. Remote Sensing of Environment, 61, 246-253

Næsset, E. (2002). Predicting forest stand characteristics with airborne scanning laser using a practical two-stage procedure and field data. Remote Sensing of Environment, 80, 88-99

Næsset, E., & Bjerknes, K.-O. (2001). Estimating tree heights and number of stems in young forest stands using airborne laser scanner data. Remote Sensing of Environment, 78, 328-340

Nellemann, C., Corcoran, E., Duarte, C.M., Valdés, L., De Young, C., Fonseca, L., & Grimsditch, G. (2009). Blue Carbon. A Rapid Response Assessment. United Nations Environment Programme, GRID-Arendal.

Nelson, R. (1997). Modeling forest canopy heights: The effects of canopy shape. Remote Sensing of Environment, 60, 327-334

Nelson, R., Ranson, K.J., Sun, G., Kimes, D.S., Kharuk, V., & Montesano, P. (2009). Estimating Siberian timber volume using MODIS and ICESat/GLAS. Remote Sensing of Environment, 113, 691-701

Nelson, R.S., R.; Krabill, W. (1988). Using airborne lasers to estimate forest canopy and stand characteristics. Journal of Forestry, 86, 31-38

Nicholls, R.J., P.P. Wong, V.R. Burkett, J.O. Codignotto, J.E. Hay, R.F. McLean, S. Ragoonaden and C.D. Woodroffe, 2007: Coastal systems and low-lying areas. Climate Change 2007: Impacts, Adaptation and Vulnerability. Contribution of Working Group II to the Fourth Assessment Report of the Intergovernmental Panel on Climate Change, M.L. Parry, O.F. Canziani, J.P. Palutikof, P.J. van der Linden and C.E. Hanson, Eds., Cambridge University Press, Cambridge, UK, 315-356

Nilsson, M. (1996). Estimation of tree heights and stand volume using an airborne lidar system. Remote Sensing of Environment, 56, 1-7

Nyman, J.A., DeLaune, R.D., Roberts, H.H., & Patrick, W.H.J. (1993). Relationship between vegetation and soil formation in a rapidly submerging coastal salt marsh. Marine Ecology Progress Series, 96, 269-279

Nyman, J.A., Walters, R.J., Delaune, R.D., & Patrick Jr, W.H. (2006). Marsh vertical accretion via vegetative growth. Estuarine, Coastal and Shelf Science, 69, 370-380

Olson, J.S., Watts, J.A., & Allison, L.J. (1983). Carbon in live vegetation of major world ecosystems. In, Live vegetation of major world ecosystems (No. DOE/NBB-0037). TN (USA): Oak Ridge National Lab

Orson, R.A., Warren, R.S., & Niering, W.A. (1998). Interpreting sea level rise and rates of vertical marsh accretion in a southern New England tidal salt marsh. Estuarine, Coastal and Shelf Science, 47, 419-429

Ozesmi, S., & Bauer, M. (2002). Satellite remote sensing of wetlands. Wetlands Ecology and Management, 10, 381-402

Pavri, F., Dailey, A., & Valentine, V. (2011). Integrating multispectral ASTER and lidar data to characterize coastal wetland landscapes in the northeastern United States. Geocarto International, 26, 647-661

Pennings, S.C., & Callaway, R.M. (1992). Salt marsh plant zonation: The relative importance of competition and physical factors. Ecology, 73, 681-690

Pethick, J.S. (1981). Long term accretion rates on tidal salt marshes. Journal of Sedimentary Research, 51, 571-577

Popescu, S.C. (2011). Lidar remote sensing. In Q. Weng (Ed.), Advances in Environmental Remote Sensing: Sensors, Algorithms, and Applications: CRC Press, NY, 57-84

Popescu, S.C., & Wynne, R.H. (2004). Seeing the trees in the forest: Using lidar and multispectral data fusion with local filtering and variable window size for estimating tree height. Photogrammetric Engineering and Remote Sensing, 70, 589-604

Popescu, S.C., Zhao, K., Neuenschwander, A., & Lin, C. (2011). Satellite lidar vs. small footprint airborne lidar: Comparing the accuracy of aboveground biomass estimates and forest structure metrics at footprint level. Remote Sensing of Environment, 115, 2786-2797

Prince, S.D., Becker-Reshef, I., & Rishmawi, K. (2009). Detection and mapping of long-term land degradation using local net production scaling: Application to Zimbabwe. Remote Sensing of Environment, 113, 1046-1057

Rango, A., Chopping, M., Ritchie, J., Havstad, K., Kustas, W., & Schmugge, T. (2000). Morphological characteristics of shrub coppice dunes in desert grasslands of southern New Mexico derived from scanning lidar. Remote Sensing of Environment, 74, 26-44

Ravens, T.M. (2006). Procuring wave information near Galveston Island. . In, Final report to the Texas coastal management program: Austin, Texas. General Land Office

Ravens, T.M., Thomas, R.C., Roberts, K.A., & Santschi, P.H. (2009). Causes of salt marsh erosion in Galveston Bay, Texas. Journal of Coastal Research, 265-272

Reddy, K.R., D'Angelo, E.M., & Harris, W.G. (1998). Biogeochemistry of wetlands. In M.E. Sumner (Ed.), Handbook of Soil Science. Boca Raton, FL, USA: CRC Press, NY, 89-119

Redfield, A.C., & Rubin, M. (1962). The age of salt marsh peat and its relation to recent changes in sea level at Barnstable, Massachusetts. Proceedings of National Academy of Science U S A., 48, 1728-1735

Richardson, A.J., & Everitt, J.H. (1992). Using spectral vegetation indices to estimate rangeland productivity. Geocarto International, 7, 63-69

Ritchie, J.C., Menenti, M., & Weltz, M.A. (1996). Measurements of land surface features using an airborne laser altimeter: the HAPEX-Sahel experiment. International Journal of Remote Sensing, 17, 3705-3724

Roman, C.T., & Daiber, F.C. (1984). Aboveground and belowground primary production dynamics of two Delaware Bay tidal marshes. Bulletin of the Torrey Botanical Club, 111, 34-41

Rosso, P.H., Ustin, S.L., & Hastings, A. (2006). Use of lidar to study changes associated with *Spartina* invasion in San Francisco Bay marshes. Remote Sensing of Environment, 100, 295-306

Rouse, J.W. (1973). Monitoring the vernal advancement and retrogradation of natural vegetation. In, NASA/GSFCT Type II Report. Greenbelt, MD, USA

Sahagian, D., & Melack, J. (1998). Global wetland distribution and functional characterization: Trace Gases and the Hydrologic Cycle. Stockholm (Sweden): International Geosphere-Biosphere Program Secretariat

Sankey, T.T., & Bond, P. (2010). Lidar-based classification of sagebrush community types. Rangeland Ecology & Management, 64, 92-98

Schmid, K.A., Hadley, B.C., & Wijekoon, N. (2011). Vertical accuracy and use of topographic lidar data in coastal marshes. Journal of Coastal Research, 116-132

Schubauer, J.P., & Hopkinson., C.S. (1984). Above- and belowground emergent macrophyte production and turnover in a coastal marsh ecosystem, Georgia. Limnology and Oceanography, 29, 1052-1065

Sellers, P.J. (1985). Canopy reflectance, photosynthesis and transpiration. International Journal of Remote Sensing, 6, 1335-1372

Shaw, J., & Ceman, J. (1999). Salt-marsh aggradation in response to late-Holocene sea-level rise at Amherst Point, Nova Scotia, Canada. The Holocene, 9, 439-451

Silliman, B.R., Grosholz, T., & Bertness, M.D.E. (2009). Human impacts on salt marshes: a global perspective. Berkeley, CA: University of California Press

Silvestri, S., Defina, A., & Marani, M. (2005). Tidal regime, salinity and salt marsh plant zonation. Estuarine, Coastal and Shelf Science, 62, 119-130

Simard, M., Rivera-Monroy, V.H., Mancera-Pineda, J.E., Castañeda-Moya, E., & Twilley, R.R. (2008). A systematic method for 3D mapping of mangrove forests based on Shuttle Radar Topography Mission elevation data, ICEsat/GLAS waveforms and field data: Application to Ciénaga Grande de Santa Marta, Colombia. Remote Sensing of Environment, 112, 2131-2144

Steininger, M.K. (2000). Satellite estimation of tropical secondary forest above-ground biomass: Data from Brazil and Bolivia. International Journal of Remote Sensing, 21, 1139-1157

Stoddart, D., Reed, D., & French, J. (1989). Understanding salt-marsh accretion, Scolt Head Island, Norfolk, England. Estuaries, 12, 228-236

Straatsma, M., & Middelkoop, H. (2007). Extracting structural characteristics of herbaceous floodplain vegetation under leaf-off conditions using airborne laser scanner data. International Journal of Remote Sensing, 28, 2447-2467

Straatsma, M.W., & Middelkoop, H. (2006). Airborne laser scanning as a tool for lowland floodplain vegetation monitoring. In R.S.E.W. Leuven, A.M.J. Ragas, A.J.M. Smits & G. Velde (Eds.), Living Rivers: Trends and Challenges in Science and Management (pp. 87-103): Springer Netherlands

Stralberg, D., Brennan, M., Callaway, J.C., Wood, J.K., Schile, L.M., Jongsomjit, D., Kelly, M., Parker, V.T., & Crooks, S. (2011). Evaluating tidal marsh sustainability in the face of sea-level rise: A hybrid modeling approach applied to San Francisco Bay. PLoS ONE, 6, 1-17

Streutker, D.R., & Glenn, N.F. (2006). Lidar measurement of sagebrush steppe vegetation heights. Remote Sensing of Environment, 102, 135-145

Syvitski, J.P.M., Kettner, A.J., Overeem, I., Hutton, E.W.H., Hannon, M.T., Brakenridge, G.R., Day, J., Vorosmarty, C., Saito, Y., Giosan, L., & Nicholls, R.J. (2009). Sinking deltas due to human activities. Nature Geoscience, 2, 681-686

Töyrä, J., Pietroniro, A., Hopkinson, C., & Kalbfleisch, W. (2003). Assessment of airborne scanning laser altimetry (lidar) in a deltaic wetland environment. Canadian Journal of Remote Sensing, 29, 718-728

Tucker, C.J. (1980). Remote sensing of leaf water content in the near infrared. Remote Sensing of Environment, 10, 23-32

Turner, R.E. (1976). Geographic variations in salt marsh macrophyte production: a review. Contributions in Marine Science, 20, 47-68

Turner, R.E., Swenson, E.M., Milan, C.S., Lee, J.M., & Oswald, T.A. (2004). Below-ground biomass in healthy and impaired salt marshes. Ecological Research, 19, 29-35

Waller, S.S., Brown, M.A., & Lewis, J.K. (1981). Factors involved in estimating green biomass by canopy spectro-reflectance measurements. Journal of Range Management, 34, 105-108

Wang, C., Menenti, M., Stoll, M.-P., Belluco, E., & Marani, M. (2007). Mapping mixed vegetation communities in salt marshes using airborne spectral data. Remote Sensing of Environment, 107, 559-570

Warren, R.S., & Niering, W.A. (1993). Vegetation change on a Northeast tidal marsh: interaction of sea-level rise and marsh accretion. Ecology, 74, 96-103

Webb, J.W., & Newling, C.J. (1985). Comparison of natural and man-made salt marshes in Galveston Bay complex, Texas. Wetlands, 4, 75-86

Weltz, M.A., Ritchie, J.C., & Fox, H.D. (1994). Comparison of laser and field measurements of vegetation height and canopy cover. Water Resources Research, 30, 1311-1319

White, W.A., & Morton, R.A. (1997). Wetland losses related to fault movement and hydrocarbon production, Southeastern Texas coast. Journal of Coastal Research, 13, 1305-1320

White, W.A., Morton, R.A., & Holmes, C.W. (2002). A comparison of factors controlling sedimentation rates and wetland loss in fluvial–deltaic systems, Texas Gulf coast. Geomorphology, 44, 47-66

White, W.A., & Tremblay, T.A. (1995). Submergence of wetlands as a result of human-induced subsidence and faulting along the upper Texas Gulf Coast. Journal of Coastal Research, 11, 788-807

Yang, S.L. (1999). Sedimentation on a growing intertidal island in the Yangtze River mouth. Estuarine Coastal Shelf Science., 49, 401-410

Yang, X. (2005). Use of lidar elevation data to construct a high resolution digital terrain model for an estuarine marsh area. International Journal of Remote Sensing, 26, 5163-5166

Yeager, K.M., Santschi, P.H., Rifai, H.S., Suarez, M.P., Brinkmeyer, R., Hung, C.-C., Schindler, K.J., Andres, M.J., & Weaver, E.A. (2007). Dioxin chronology and fluxes in sediments of the Houston Ship Channel, Texas: Influences of non-steady-state sediment transport and total organic carbon. Environmental Science & Technology, 41, 5291-5298

Zolkos, S.G., Goetz, S.J., & Dubayah, R. (2013). A meta-analysis of terrestrial aboveground biomass estimation using lidar remote sensing. Remote Sensing of Environment, 128, 289-298